HASP Student Payload Application for 2018

Payload Title: Sheffield University Nova Balloon Lifted Telescope		
Institution: The University of Sheffield		
Payload Class: LARGE		Submit Date: 15.12.2017
Project Abstract: Sun surveillance from the ground is often difficult as the thick atmosphere of the Earth blocks and distorts much of the incoming light. Learning about the Sun is critical in modern society, when solar flares have the potential to cripple telecommunication and global navigation systems. In the UK alone, €22mn was invested in the Space Situational Awareness program emphasising the need to better understand and predict solar events. Project SunbYte (Sheffield University Nova Balloon Lifted Telescope) aims to revolutionise the industry of solar observations by using a high-altitude balloon to lift a telescope to an altitude of 25-35km, where SunbYte has the potential to capture images of much better quality. As the existing ground and space telescopes are large, complex and expensive, the number of scientists who have access to such resources are quite limited. Even though experimental studies using high-altitude balloon telescopes have been previously conducted, these are, in terms of cost, inaccessible to many mainstream research institutions across the world. Combining the latest practices in manufacturing, astrophysics science and engineering, the team aims to deliver a low cost high quality method of imaging the Sun. The experiment was launched on BEXUS 25 from ESRANGE, Sweden in Oct 2017 as part of the REXUS/BEXUS programme. This document will discuss the new design for launch on HASP based on the lessons learnt.		
Team Name: SunbYte		Team or Project Website http://sunbyte.group.shef.ac.uk
Student Leader Contact Information:		Faculty Advisor Contact Information:
Name:	Iakov Bobrov	Dr. Viktor Fedun
Department:	Department of Aerospace Engineering	Department of Automatic Control and Systems Engineering
Mailing Address:	Department of Automatic Control and Systems Engineering University of Sheffield	Department of Automatic Control and Systems Engineering University of Sheffield
City, State, Zip code:	S1 3JD, Sheffield	S1 3JD, Sheffield
e-mail:	ibobrov1@sheffield.ac.uk	v.fedun@sheffield.ac.uk
Office Telephone:	+447557381923	+44 114 2225197
Mobile Telephone:	+44 7554902627	+44 114 2225197

Contents

1. Introduction

1.1. Scientific/Technical Background

The Sun is the most important source of energy for the Earth and it is essential that we keep
it under surveillance in order to understand how any changes will affect our planet.
In 1895, a solar coronal mass ejection hit the Earth's magnetosphere and caused Auroras to appear as far South as the Caribbean. In 1989, a geomagnetic storm took out much of Quebec's electricity grid plunging the country into chaos. If such an event were to occur nowadays, where delicate electronic devices a ect important aspects of our lives such as security, the outcome would be even more devastating. In 2012, there was a solar storm of equal magnitude as the one that occurred in 1895 but luckily missed the Earth. Given the impact of these threatening events former U.S. President Barack Obama issued an executive order calling for preparations against solar flares in October 2016 [1]. Solar storms are one of the most significant outer space threats to normal life - hence the need for development of low cost access to monitoring of the Sun is imperative.

1.2. Mission Statement

Current Earth-based solar telescopes are very expensive in part due to the large and costly equipment required for compensation of astronomical "seeing" (Refraction and scattering distortions caused by Earth's atmosphere). This reduces the quality of images taken. Whilst space-based telescopes can avoid astronomical seeing and astronomical extinction (absorption of electromagnetic radiation in the ultraviolet, X-ray and gamma wavelengths), these require expensive rocket launchers and are practically impossible to modify or modernise once launched into orbit.
Traditionally, the best solution has been to locate observatories as high as possible to minimise the thickness of atmosphere. Lucky imaging is also used to capture moments when above the thick atmosphere . Combining these conventional ideas, project SunbYte aims to use high altitude balloons to hoist a telescope higher than ever to the edges of the Earth's atmosphere at 36,000m altitude. High frame rate lucky imaging will further increase the probability of acquiring scientifically worthwhile images.

1.3. Experiment Objectives

1. Primary objective: Track and image the Sun in H-alpha line.
2. Secondary objectives: Acquire focused solar images to demonstrate scientific potential.
3. Tertiary objectives: Promote and increase space engineering studies in "aerospace engineering" courses across the country.

1.4. Experiment Concept

Based on the objectives laid out in section 1.3, a full list of derived function, performance, design and operational requirements can be found in Section 1 of the appendix. To assess the validity of the design against these requirements, a test plan was established and can be found in Section 2 of the appendix.
In order to locate and track the Sun we have 2 tracking cameras attached to the telescope tube:

a) **Wide-field tracker**: using a coned mirror to provide 360 degree images that will enable the machine to determine the direction to slew the telescope to aim at the sun.
b) **Precise tracker**: using a high quality camera with narrower field of view to precisely track the sun in real-time.

Both of these cameras will have be connected to the tracking Raspberry Pi and will find the sun in the images using code developed with OpenCV in Python to detect the bright disc of the sun. Adding neutral solar filters to the cameras (99.99% absorption) will ensure that only the disc of the sun is visible in images. Once located, instructions are sent from the Raspberry Pi to the Arduino motor controller to precisely position the telescope.
The science data acquisition camera will be a USB camera attached to the prime focus of the telescope tube, this will be connected to the science acquisition Raspberry Pi and is expected to capture images of 1920x1080 at a rate of upto ~15 FPS (limited by the speed of the Raspberry Pi). The images will be saved to an SD card for post-flight analysis and the system will intermittently launch a focusing routine, adjusting the focus of the telescope and comparing images, to ensure the images are sharp for the direction of the flight.
A selection of highly cropped and reduced images will be intermittently transmitted to the ground station from each of the 3 cameras during flight, to verify target and focus of the telescope.

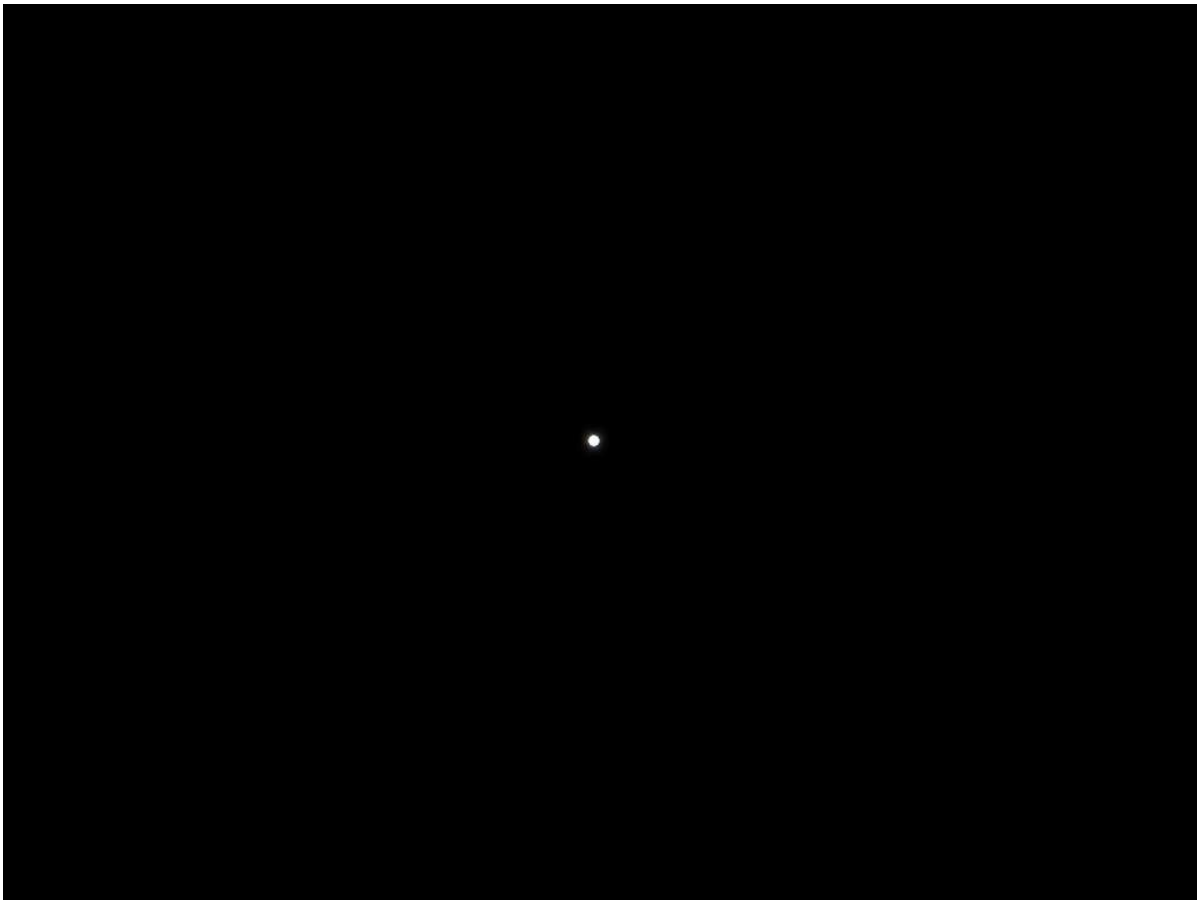

Images of the sun as taken by a Raspberry Pi Camera Module v2.1 with Baader Planetarium AstroSolar Solar Filter film. The disc of the sun is clear and easy to track.

Team Details

1.4.1. Contact point

Name: Iakov Bobrov (team leader)
Address:
Department of Automatic Control and Systems Engineering
University of Sheffield
S1 3JD, UK
Tel: +447554902627
E-mail: ibobrov1@sheffield.ac.uk
Team E-mail: SunbYte@sheffield.ac.uk

1.4.2. Team members

Name	Institution	Responsibility
Iakov Bobrov, 2nd year Aerospace BEng	University of Sheffield	Team leader and overall project management
Yun-Hang Cho, 2nd year Civil Engineering PhD	University of Sheffield	Systems Engineering support and mentorship
Alex Hamilton, 2nd year Physics PhD	University of Hull	Software team leader
Joycelyn Fontanilla 2nd year Chemical Engineering MEng	University of Sheffield	Mechanical team leader
Alex Menzies 3rd year Mechanical BEng	University of Sheffield	CAD modelling and Thermal Analysis
Ana-Maria Badilita, 2nd year Aerospace BEng	University of Sheffield	Outreach, Finite Element Analysis
Mate Lukacs 2nd year Mechanical MEng	University of Sheffield	Finite Element Analysis and documentation
George Robinson, 2nd year Aerospace MEng	University of Sheffield	Outreach and Thermal Analysis
Gianni Sin Yi Heung 1st year Telecommunications MSc	The University of Hong Kong	Electronics, image focusing and telemetry

It is anticipated that between 4 and 6 students will participate in integration at CSBF and between 5 and 8 students will participate in flight operations at Ft. Sumner.

2. Project Planning

The project is currently managed on a day-to-day basis by the sub-team leaders. As principal participant, the team leader is responsible for the overall project management and direction. The project will be supervised by the Academic Lead with mentoring support to conduct internal project reviews which will highlight the progress made, and discuss the necessary steps for further advancement of the project. The team leader is responsible for the meeting of obligations of the Project (administrative, technical and financial), monitoring progress, ensuring work is delivered within schedule, chairing, and reporting of project meetings in order ensure a good collaboration between team sub-divisions and partners.

At the operational level, each task has a responsible student lead (supported by an Academic Advisor when necessary) for the day-to-day management of the activity to be carried out. His/her main responsibility includes monitoring of the work carried out by their teams within the project and organisation of the deliverables.

Work package management is planned and monitored through Gantt charts and a gate review system. Weekly reviews have been conducted and will continue to be conducted as the project goes through the phases. Shared Google docs, email lists, LaTeX documents, Overleaf, Slack, Skype and Facebook are the main forms of cooperative work and provide an effective communication tool.

The team leader with the assistance from Dr. V. Fedun, (Lecturer in Dept. of Automatic Control and Systems Engineering at the University of Sheffield) ensures that the project is managed on a day-to-day basis and is responsible for the successful running and delivery of the following tasks:

1. Meeting the contractual obligations of the project (financial, administrative, and scientific).
2. Monitoring the progress of the project and ensuring deliverables are met.
3. Organising, chairing and reporting of project meetings.
4. Ensuring good, timely communications between the members of the team.

Advisors and Senior Researchers participate and assist the students involved in the project in subjects such as equipment, installation and algorithms.

2.1. Schedule

The project can be divided into 7 main phases; these are shown in the table below alongside with non-productive periods, such as exams and holidays.
The table below explains some of the key activities taking place during each stage.

Phase	Name	Description
0	Concept	Develop concept and feasibility analysis of mission.
A	Preliminary Design	Develop requirements and first design.
B	Detailed Design	Build test prototypes to validate and develop design.
C	Manufacturing	Manufacture, test and assembly of flight model
D	Integration	Integrate payload into launch vehicle.
E	Launch	Launch activities, monitor status, downlink data, uplink commands.
F	Post Porecssing	Analyse data and compare against industry standards.

Figure 2.1.1. – Legend for Gantt Chart

Using the work breakdown structure, the Gantt chart below shows a detailed breakdown of the tasks undertaken by each sub-team during the current phase (detailed design) and the periods of when the activities began and will finish.

	2017			2018											
	Oct	Nov	Dec	Jan	Feb	Mar	Apr	May	Jun	Jul	Aug	Sep	Oct	Nov	Dec
Notes	BESUX 25 Launch			Exam				Exam	Holiday						
Phase 0	Concept														
Phase A		Preliminary Design													
Phase B				Detailed Designs											
Phase C						Manufacturing, AIT									
Phase D											Integrati on				
Phase E												Launch			
Phase F													Post processing		

Figure 2.1.2. – Gantt Chart

2.2. Resources

This budget includes spare elements to account for possible loss during testing and/or integration stages. The total cost of electrical sub-system was evaluated to be £14,324.63 ($19,195), cost of mechanical sub-system was £2,888.68 (3,870.8312$), cost of optics sub-system was £14,664.83 ($19,651). The full breakdown of this can be found in section 3.1 of the Appendix.
So far we have received funding in the amount of £41,815 (55,703$) as seen in section 3.2 of the Appendix.

2.3. Risk

A list of safety, project and technical risks can be found in the appendix 6.2. Actions to reduce these risks are stated where necessary.

3. Experiment description

3.1. Experiment setup

Our experiment can be classified into three sections, optics, electronics and mechanical structure.

3.1.1. The Solar Telescope and Camera System

Because of considerations outlined below, the telescope design will be based on Maksutov Cassegrain reflector design.

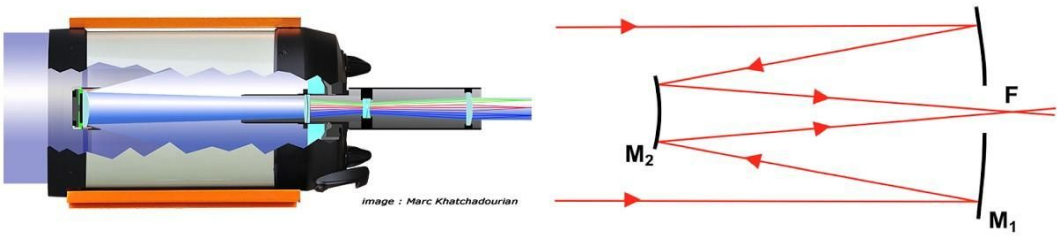

Figure 3.1.1.1. – Telescope configuration

This design differs from the classic Cassegrain design by having a corrective negative lens at the front of the telescope to correct for the off-axis aberrations. The design has a relatively narrow field of view making it suitable for solar observations.

1. Target considerations: The Sun subtends an angle of approximately 1,865 arc seconds (0.52 degrees) to an observer on the Earth. The diameter of the Sun is 1.392 $*$ 10^9 m (864,949 miles).
2. Angle of view: The telescope will be limited to making observations of the Sun only and therefore it will be acceptable to use an optical system with a narrow field of view.
3. Size of system: The Meade ETX 125 maksutov-cassegrain telescope, aperture 125 mm primary mirror to image onto a CCD sensor
4. Limits to telescope resolution:
    - Atmospheric distortion. At ground level, atmospheric distortion limits telescope resolution depending on location. In this application, atmospheric distortion is minimised.
    - Diffraction. The resolution of the telescope is limited by the size of the primary reflecting optic. This may be calculated as: **Angular resolution (radians) = 1.22 x wavelength / optic diameter**. A 125 mm primary optic offers a 1.1 arcsecond resolution for light 550 nm. (1 radian = 206,265 arcsec.)
    - Sensor and pixel size. The angle of view is determined by: **FoV = arctan (sensor size / focal length)**.
    - Likewise sensor resolution is limited by: **Sensor resolution = arctan (pixel spacing size / focal length)**. The imaging sensor will be placed at the focal point of the mirror assembly.
5. Environmental considerations
    - Temperature variations: It is expected that the telescope will suffer an extreme range of temperatures. Due consideration will be given to thermal expansion (contraction) which may impact the primary and secondary mirror alignment as well as the positioning of the imaging sensor at the focal point of the telescope.

- Condensation of water vapour: Consideration will also be given to the possibility that water vapour may condense on the optics at altitude due to low temperatures.

6. The telescope will have a neutral density solar filter to block the majority (99.99%) of light to protect optics and sensors.

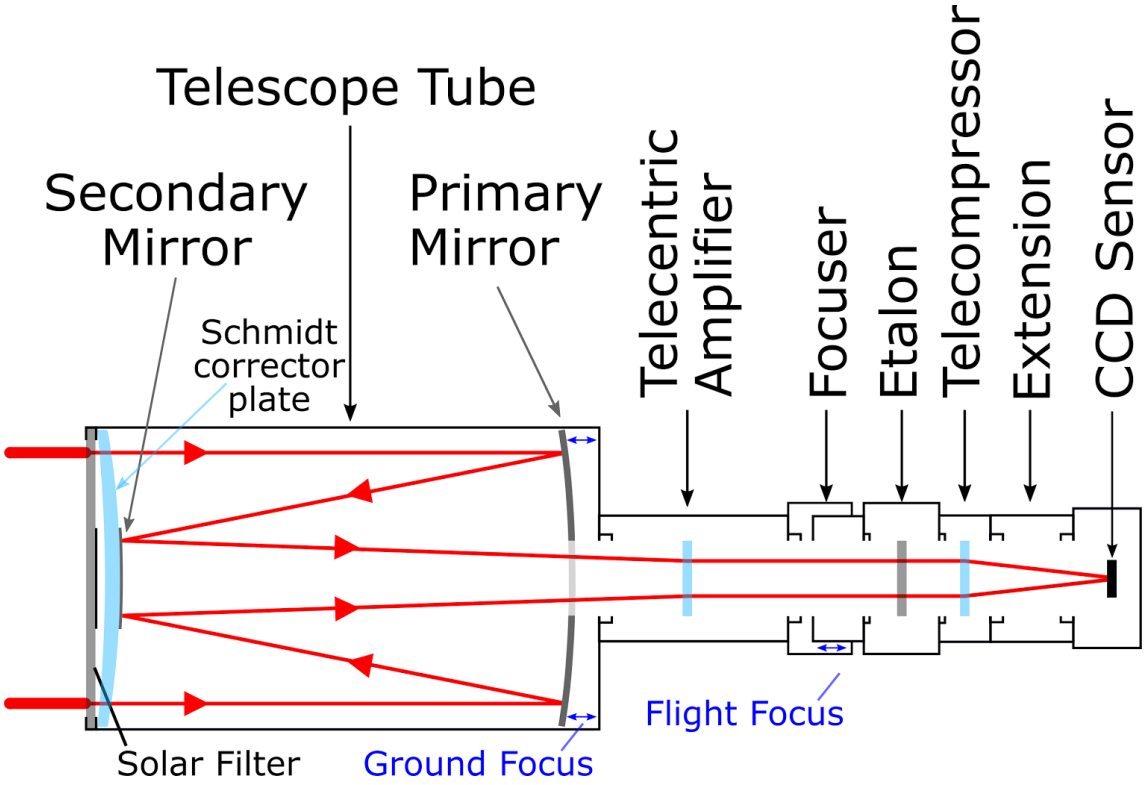

Figure 3.1.1.2 – Schematic of optical system

3.1.2. The tracking and control system

The team will develop a two-stage tracking system for pinpointing the location of the Sun in real-time.

It will consists of correcting the position of the Sun as the geometric distance to the centre of the image acquired. The vector to the centroid will be passed to the control team who will create a 2 axis attitude control system using stepper motors. This is further discussed and explained later in this section.

During most testing the hardware platform of choice has been a Raspberry Pi due to ease of implementation, however it is possible that this device will be substituted in the near future by a more powerful platform.

3.1.3. The data storage system

Images and data recorded by the telescope imager will be stored onto a SD micro card in the science acquisition Raspberry Pi. This will be downloaded after retrieval for analysis. All systems will be tested for low temperatures, outgassing and other space hazards such as atomic oxygen.

We want to obtain images of the Sun using the Balmer series H-alpha deep-red visible spectral line at wavelength 656.28 nm. Using a 125 mm diameter aperture and effective 1900 mm focal length, we will connect this onto a ZWO ASI120MM sensor with an H-alpha etalon/filter.

3.2. Experiment Interfaces

3.2.1. Mechanical

Positioning with respect to the gondola

It is intended to mount the telescope on one of the large slots allocated on the gondola. The configuration of the support can be seen in Figure 3.2.1.1.

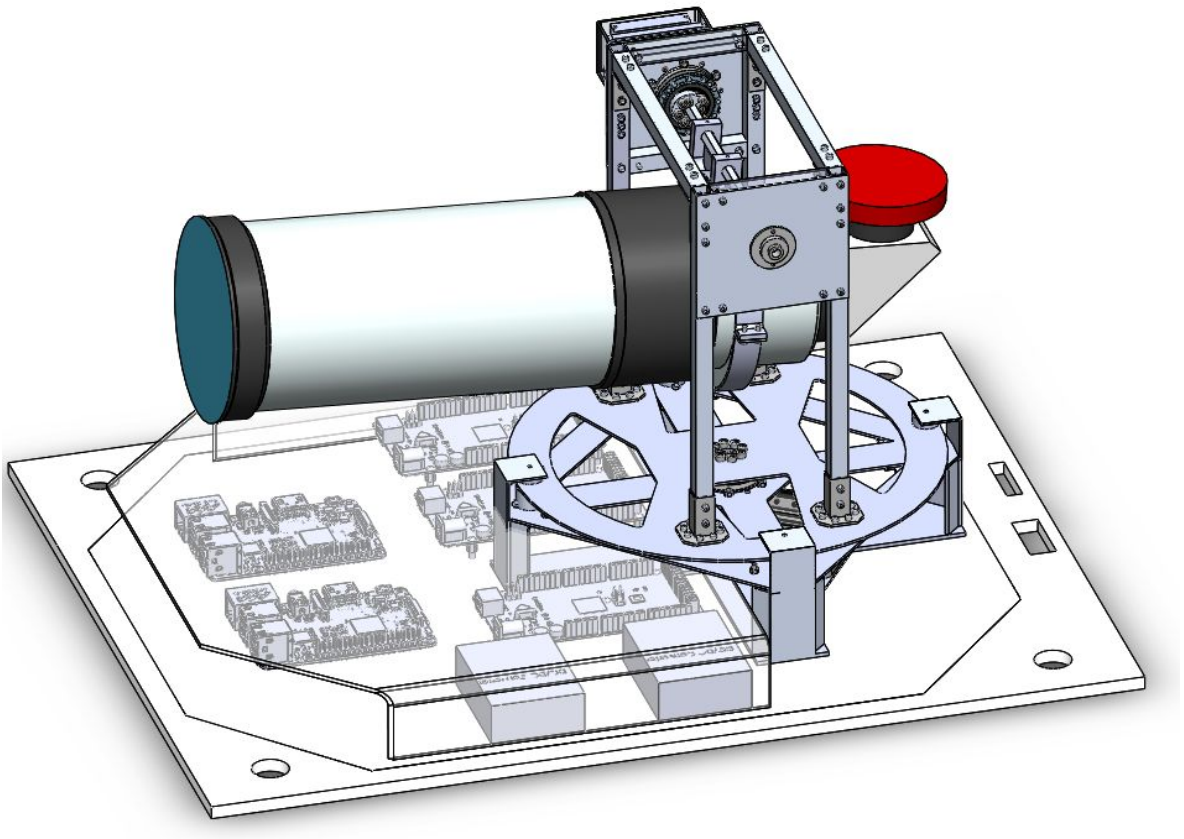

Figure 3.2.1.1. – Positioning with respect to the gondola

Bolts will be used to secure the structure onto the PVC board provided. The final size will be determined after additional structural calculations and testing. Dimensions can be found in appendix Section 4.1.1.

3.2.2. Electrical

Due to the space limitation imposed by the HASP regulations [2] the electronic components and systems will be mounted, with standoff screws and insulation, to the PVC mounting plate provided to us. It can be seen in Figure 3.2.2.1. Previously the electronics box had 3 layers.

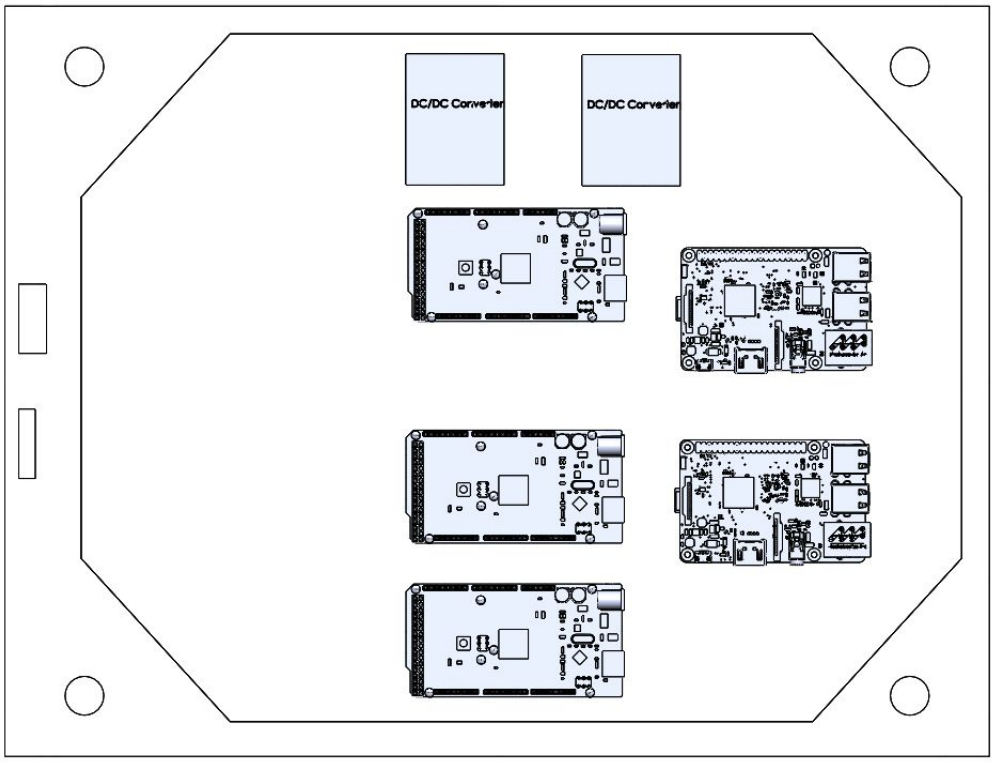

Figure 3.2.2.1. – Electronics system

Table 3.2.2.1 - Electrical Interfaces applicable to HASP

HASP Electrical Interfaces	Yes
Data rate - downlink:	4 kbps
Data rate - uplink	2 bytes when needed
Peak power (or current) consumption:	75 W or 4.6 A
Average power (or current) consumption:	50 W or 2.5 A

3.2.3. Inside the Electronics Box

Usage of HASP Serial

The system should be able to run autonomously once switched on, automatically finding and tracking the sun with the ability to focus on the fly. However to improve the reliability and enable troubleshooting during flight, the serial of the tracking Raspberry Pi will be accessible with a terminal via the HASP serial interface [2].

Computer Interconnects

The Raspberry Pi computers will be connected together via a direct network connection, using a crossover cable, this will allow the scientific acquisition Raspberry Pi to be accessed via the tracking Raspberry Pi terminal. As a result, it will allowing remote access to reconfigure and even reboot either computer during flight.

A small number of highly compressed and cropped images can also be downloaded to the ground station during flight using this connection, to give us a delayed view of how well the tracking and focusing is working.

3.3. Experiment Components

Table 3.3.1. – Dimensions and mass of the mechanical structure

Experiment mass	9.7kg
Experiment dimensions	300 x 388 x 300* mm
Experiment footprint area	0.116 m^2
Experiment volume	0.0349 m^3

Due to the nature of the experiment, the structure is not entirely static. Ideally the telescope would be able to have total freedom to be angled up to a pitch of 65 degrees, reflecting the maximum pitch of the sun in the sky that is expected. It should be noted that due to the duration of the flight, SunbYte will have ample opportunity to gather data when the sun is lower in the sky, and therefore that the hard imposition of the height restriction would only reduce the fraction of flight time during which the experiment could gather data.
SunbYte would wish to discuss with neighbouring experiments the potential for our telescope to stray beyond the allocated experiment dimensions.

Table 3.3.2. – Dimensions and mass of the electronics box

Experiment mass	3.2kg (including the electronics)
Experiment dimensions	330 x 255 x 35 mm
Experiment footprint area	0.08415 m^2
Experiment volume	0.002945 m^3

Table 3.3.3 – Mass of various components

Actuators	
Raspberry Pi 3	0.2kg
Electrical motors (x2)	2 x 0.5kg
Driver hardware including heat sinks (x2)	2 x 0.03kg
DC-DC converters (x2)	<0.5kg
Actuator Sub-Total:	**<1.76kg**
Image Acquisition System	
Raspberry Pi 3	0.2kg
USB Webcam	0.5kg
Acquisition Sub-Total:	<**0.7kg**
Optics	
Telescope tube	<4kg
Additional optics	0.5kg
Tracking cameras	<0.1kg
Optics Sub-Total:	<**4.6kg**
Mechanical structure	
Gimbal structure	<3.9kg
Electronic box	<0.5kg
Nuts and bolts	<0.61kg
Mechanical structure Sub-Total:	<**5.1kg**
Total	<**12.5kg**

3.4. Mechanical Design

3.4.1. Telescope

In order to evaluate the focus control is working suitably, a resolution of <2 arcsec at the vacuum wavelength of H-alpha line core (656.28 nm) is required. The choice of the line is based on the following factors:

- The sensitivity of most CCD/CMOS cameras are close to its maximum at this wavelength;
- This wavelength is close to the peak of the Planck function, which approximately describes the solar radiation spectrum as a black body radiation with the effective temperature of 5700 K;
- H-alpha line core is formed mostly in the solar chromosphere with some lower corona influence, making it especially attractive for scientific applications;
- H-alpha line core etalons are commercially available as they are commonly used in amateur astronomy.

1 arcsec resolution is achieved by a telescope with a primary mirror of 80 mm diameter, which its diffraction-limited resolution is 0.825 arcsec at the required wavelength. It is preferential to use bursts of short exposures for solar imaging to reduce impact of

imperfections in the stabilisation system. This will reduce the blur caused by the residual gondola movement, and application of standard solar imaging processing software (SunPy and IDL SolarSoft) to the obtained data will eliminate shifts and align images, further improving the effective resolution. Taking into account the broad frequency spectrum of gondola motions, short exposures of 0.05 seconds are needed to maintain sufficient image quality. However, short exposures lead to less light arriving at sensor. Therefore, a highly sensitive CCD such as the ZWO ASI120mm (mono) could be used. This is shown as an example in the CAD model.

3.4.2. Gimbal

After consultation with a harmonic drive company, we decided on the HFUC-20-2UH as per their suggestion. The HFUC-20-2UH is already available in stock which is preferable considering the project timeline. The current model meets the experiment requirements and shall be compatible with the motors in hand provided the use if a sleeve to ensure a proper connection between the motor and the harmonic drive.

A telescope shaft with a hexagonal cross section was implemented. The hexagonal cross section prevents slippage between the telescope clamp and shaft. The new selected harmonic drives have already incorporated in their design bearings at the output which support the platform in a radial direction and prevent the misalignment between the motor and the gear.

Two of the diagonal struts which connects to the platform have been shifted down to reduce the stress concentration due to the bolt holes.

Gimbal Platform

Fixed Plate

The fixed square-shaped plate with the central motor compartment is shown on Figure 4.23.

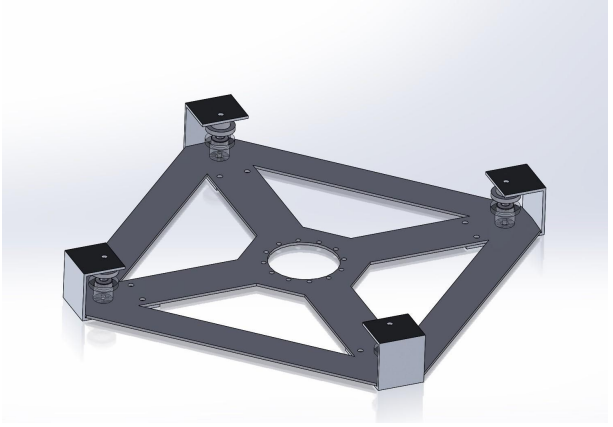

Figure 3.4.2.1. – Fixed Plate

The platform increases vibrational stability of the rotating plate and even distribution of the mass. It was designed to prevent any uncontrolled motion of the rotating platform and to maintain low weight.

C-clamps

The height of the clamp been reduced due to platform motor being changed from between the two platform to below the fixed platform. The original C-clamps shown in Figure 4.24 are to ensure that the rotating platform will have negligible vibrational impact, if any vertical motion occurs during operation.

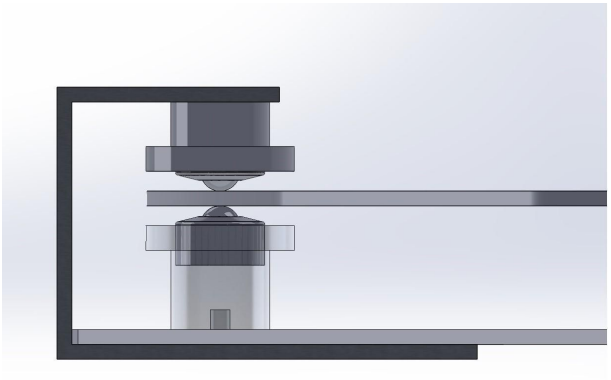

Figure 3.4.2.2. – C-clamp

The cross-section of the bearing supports was changed to reduce weight and ease manufacture. The bearing supports will be used to house steel ball transfer units which enable the rotation of the platform.

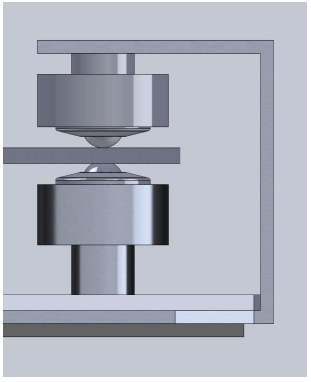

Figure 3.4.2.3. – Refined C-clamp

The platform assembly is presented in Figure 3.4.2.4., 3.4.2.5. and 3.4.2.6.

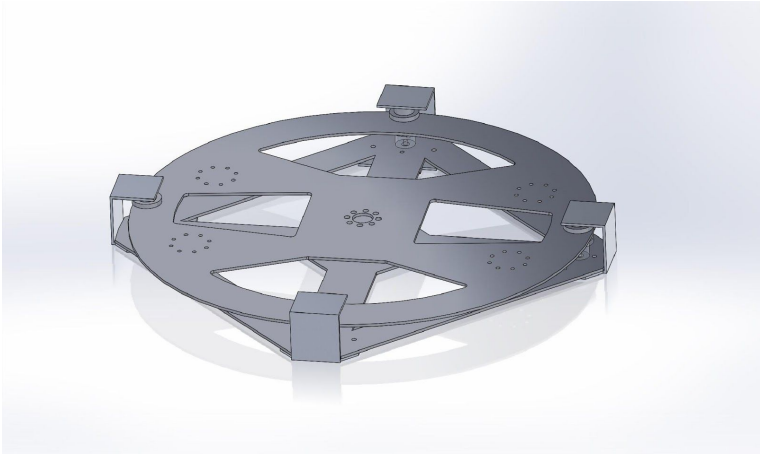

Figure 3.4.2.4. – Platform Assembly

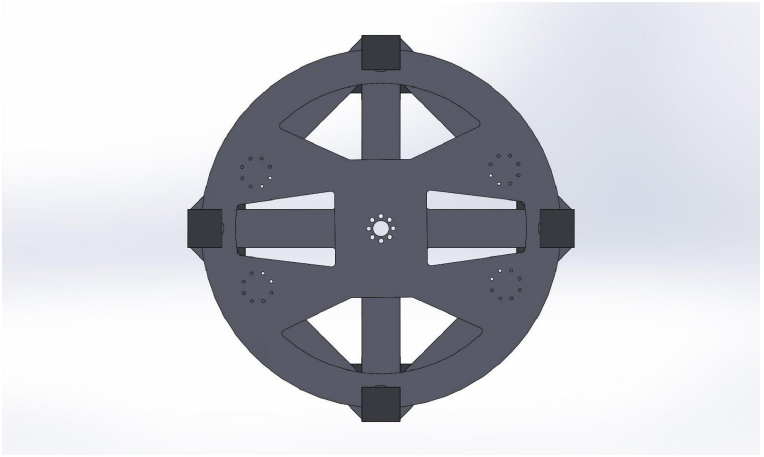

Figure 3.4.2.5. – Platform Assembly - Top View

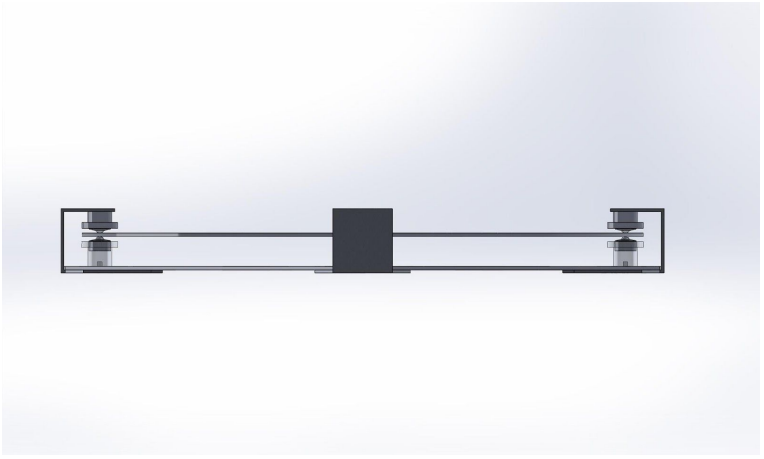

Figure 3.4.2.6. – Platform Assembly - Side View

Pitch Motor Housing

The motor driving the pitch of the telescope is to be mounted on one of the side supports. The housing consists of two components; formed from bending 2.5mm aluminium alloy 6082 plates into the specified geometries. The driver is to be mounted centrally on the larger part and the motor to sit on the opposite face on the other piece. Cables are to be fitted to connect the motor and the driver and exit the base plate.

The pitch motor casing is made up of a bracket that is screwed onto the plate of the vertical support. There will be a hole for a Dsub 9 connector on the bracket. The motor is mounted onto a curved panel. Strips of aluminium metal sheet serve to reinforce the thermal insulation, which will be 3cm of white PE foam encasing the outside. Aluminized mylar foil which will be wrapped around the foam insulation for protection against radiation.

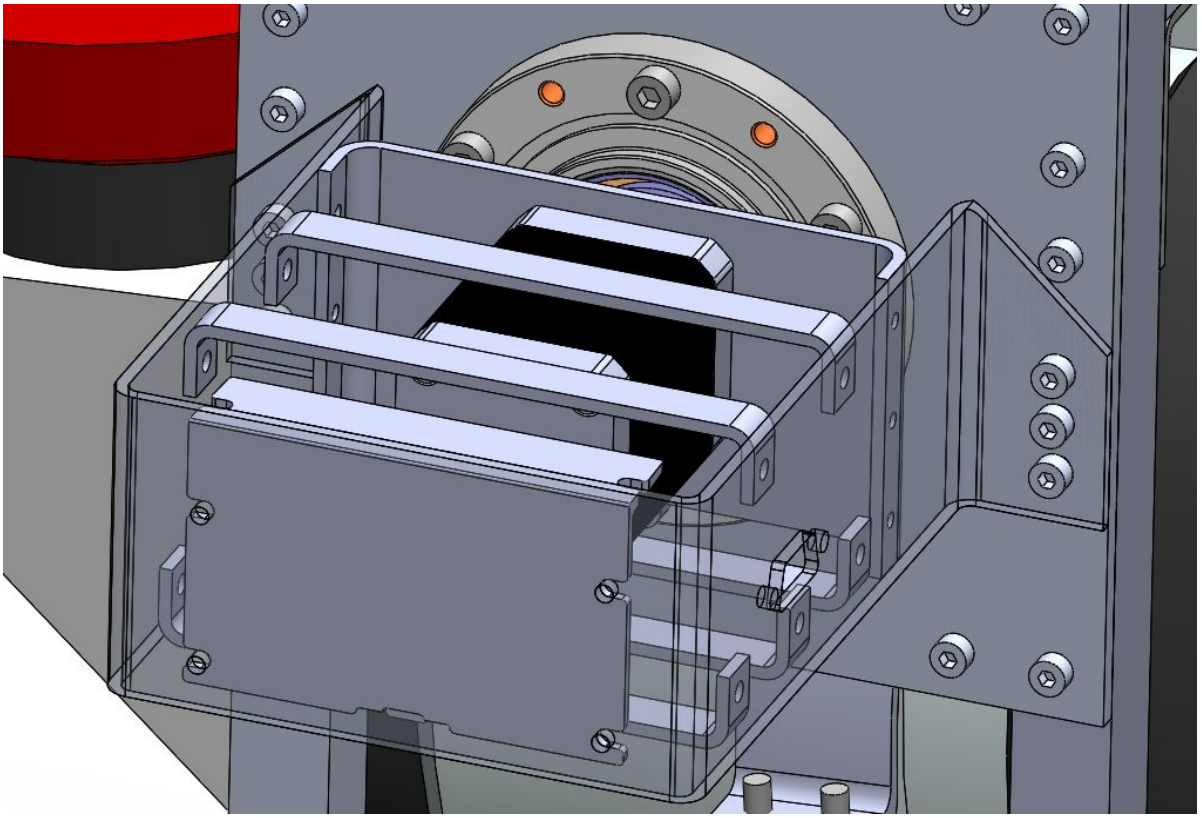

Figure 3.4.2.7. – Close-up 3D CAD of pitch motor housing.

Yaw Motor Housing

The motor driving the yaw of the telescope was to be mounted on the top of the mounting plate. The casing will have to be mounted at an angle to the sides of the 40mm strut due to the limiting space. The manufacturing procedure was to follows a similar process as the pitch motor housing, however the assembly is process is different. The main body of the casing were to be made by welding sheets of aluminium 6082 at 90 degrees to each other. The underside of the casing was to be attached using nuts and bolts at the two ends. As with the Pitch motor housing, an airtight seal is not required so there will be no silicone sealant.

Upon further consideration and consultation, the design has been modified so that the sides of the motor housing are riveted together.

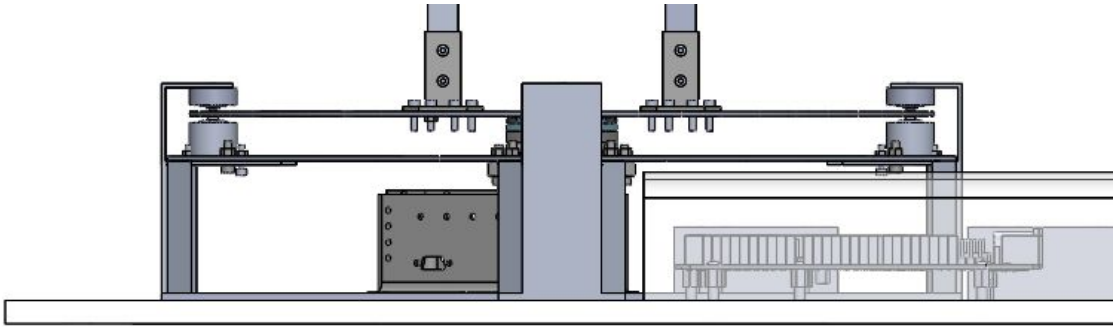

Figure 3.4.2.8. – Yaw motor housing on assembly with D sub 9 slot. This will be used to connect a cable to the pitch motor.

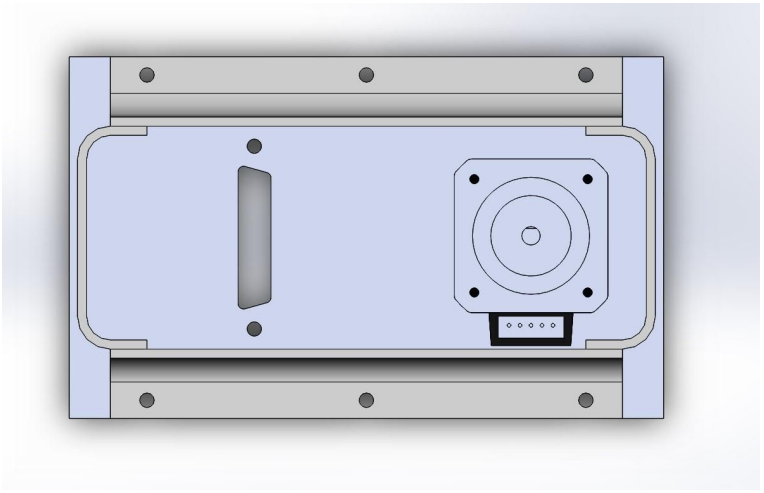

Figure 3.4.2.9. – Yaw motor housing with Dsub 25 slot shown. This will be used to connect a cable to the electronics box.

Telescope clamps attached to the shaft and bearings are shown in Figure 3.4.2.10.
The telescope clamps were altered so that there was a gap between bolted faces to allow for stiffer fastening and greater adjustability.

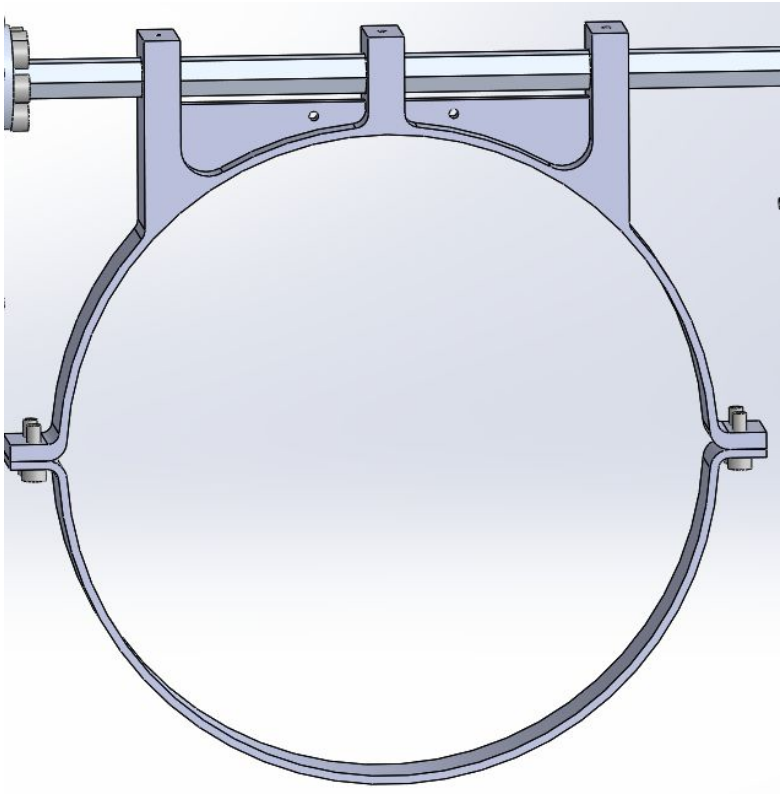

Figure 3.4.2.10. – Telescope clamps

After further design consideration and design review under the guidance of the technicians supervising our progress, the team members have redesigned the telescope clamp so that can be manufactured using the wire EDM technique. The current design is expected to be more rigid and provide a required stiffness so that the telescope can be easily rotated about the axis of motion considered as the centre of mass is situated right next to the point of attachment of the clamp on the telescope body.

Pi Camera Mount

The Pi camera and Adafruit mount is going to be made completely from PLA, this is not only because it is lightweight so it will not weigh down the front of the camera, because it is made from plastic it will not affect the adafruit magnetic compass so the readings will be precise. This enclosure will be covered in PE foam on all sides except the bottom and the front where the camera is located.

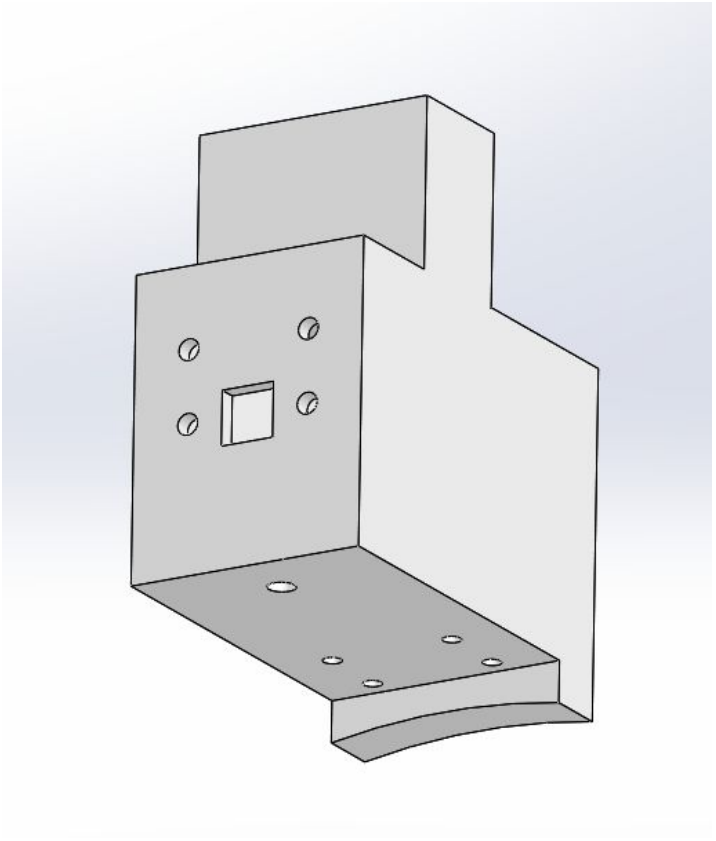

Figure 3.4.2.11. – Pi camera and Adafruit

3.4.3. Motor shaft adapter

As the motor cannot be connected directly to the harmonic drive, a shaft adapter has been designed to interface between the two components.
The motor adaptor is intended to be 3D printed using as primary material, titanium. This is going to be facilitated by one of our sponsors, the Centre for Advanced Additive Manufacturing, who are also providing guidance in terms of using and integrating other possible 3D printed parts in our design.

3.5. Electronics Design

The main goal of the electronic components is to provide a platform for the software that allows an effective tracking of the Sun and correct adjustment of the telescope. During the entire duration of this project the electronic components selected have changed continuously, this has been possible due to a total lack of custom electronic designs. We rely entirely on off-the-shelf components already integrated in an easy to use platform.
The elements have been summarized below.

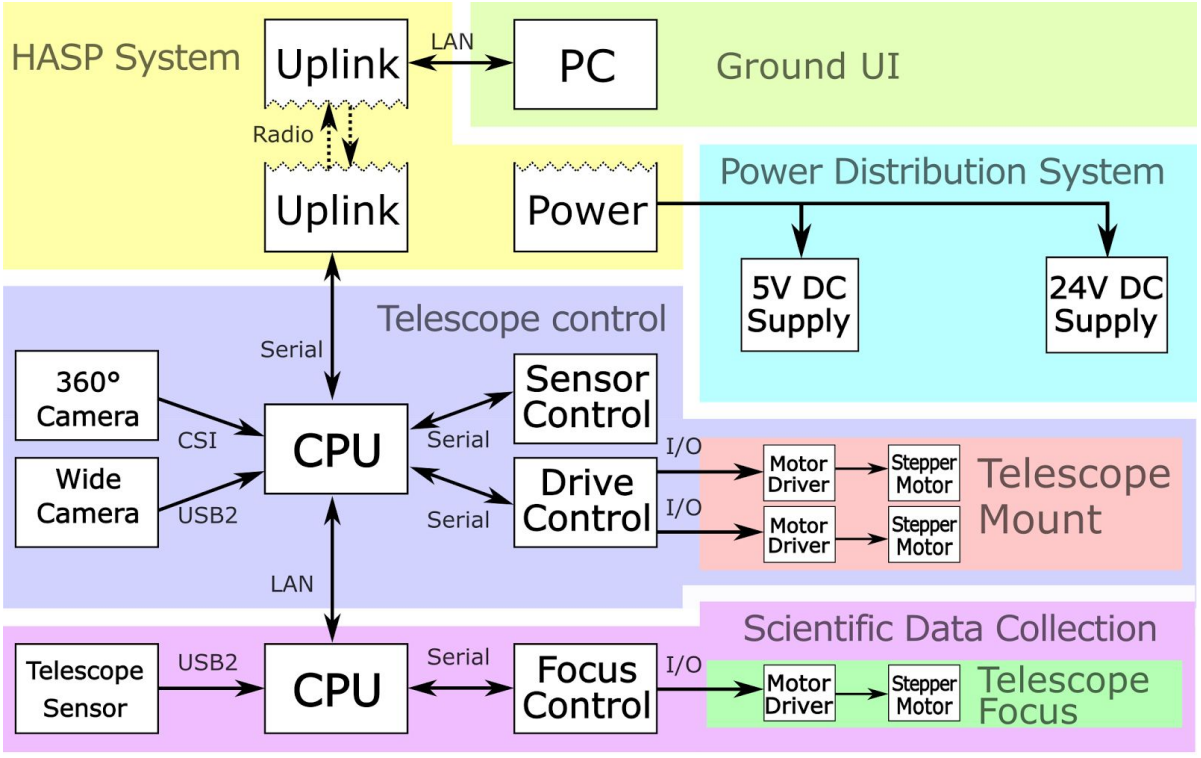

Figure 3.5.1 – Overall electrical architecture interface.

In its current state, the entire system is composed of a Raspberry Pi in charge of overall control of the experiment and Sun tracking through a PI camera, 2/3 Arduino-based EtherMegas for motor control and monitoring sensors, a second Raspberry Pi for data acquisition with our CCD camera, 2 high resolution stepper motors, 1 focusing system, 3 DC/DC converters, 2 CVK series drivers for controlling the motors and several sensors for control and monitoring including at least 3 current sensors that will allow monitoring power and at least 2 Adafruit 9 DOF sensors which will be employed to calculate the orientation of the gimbal/telescope.

- **Arduino Mega** The Arduino is the base for motor control. Additionally, it will provide some extra ports for sensors. During testing each bipolar stepper motor has required at least 4 of the 14 available digital I/O ports. Since the motors will be

substituted in the future by 5 phase motors, the final employed Arduino microcontroller platform will most likely be Arduino MEGA opposed to the Arduino UNO used during most testing up to date. The reason for this change is the far superior amount of available digital and analogue connections.

- **Raspberry PI v3** The Raspberry PI v3 is the brain of proposed Sun tracking and position estimation algorithms. It provides communication with the ground station as well as manages all interfaces between electronic devices.
- **Webcam Pi Camera v2 or Logitech c920** Linux allows for the use of many webcams. We are evaluating the Pi camera as an easy to use device specifically designed to be used together with a Raspberry Pi. The only problem it could present is the relatively weak CSI (camera serial interface) bus connector which luckily can be converted into a more robust connector such as HDMI which allows for easier implementation of a fixing solution involving screws. The connection between camera and raspberry pi board can be done using CSI/HDMI & HDMI/CSI adapters and a more robust against twisting HDMI cable. The video mode resolution is 640 x 480 pixels. Alternatively, we also have a Logitech c920 to test, providing 1080P@30 Hz with hardware MPEG compression over USB2.0.
- **Stepper Motors** As seen in the ”Appendix C - Electrical testing”, the stepper motors employed during the early stages of testing were bipolar Nema 16, with 1.8 degrees per step. Due to incredibly demanding accuracy, these motors have now been substituted by 5-phase stepper motors from ”Orientalmotor”which allow for as little as 0.36 degrees per step by default. In addition, a method of operation known as micro-stepping will be carried out through the CVK series drivers allowing for as little as 0.00288 degrees per step to reduce the need of a very precise gearbox / harmonic drive. All elements involved have already been acquired and tested and the method described is an industry proven solution. Additionally, as shown at the Electrical testing appendix, the motors are capable of working at cold conditions of at least -18 °C.
- **Motor** The motor will be used to drive the focuser, which will be the TS-Optics 2”Non Rotating Helical Focuser with M48 connection.
- **DC/DC Converters** Due to the fact that, regarding power testing is currently carried out by use of several DC power supplies, the final DC/DC converters have not been selected. However the needed conditions are at this point almost certain with 3 converters. Two of them will deliver 12 and 5V supply to electronic devices located inside the gondola while the other one will deliver a 12V supply both to the stepper motors and motor as well as the sCMOS camera.
- **Adafruit 9 DoF** This element is particularly useful to provide basic telemetry as well as to provide the necessary information for one of the Sun locating solutions based on position of the gondola with respect to the magnetic pole of The Earth and the date/time during the HASP flight. It includes Gyroscope, Magnetometer, Barometer and Thermometer. This element will be located right on top of the aluminium box containing the electronics to avoid possible interferences as well as on the gimbal and the telescope to avoid the effect of the permanent magnets employed by the Hamburg team inside the gondola and to compare the information and gain a further insight into the orientation of our telescope. The box itself should not interfere with the magnetic readings given that it is not a ferromagnetic material and thus it wouldn‘t become a Faraday cage, however, eddy currents travelling through the aluminium could shield it from reading outside magnetic fields.

3.5.1. Stability/Actuation System

The control loop is represented in a simplified manner keeping only the relevant components in the Sun tracking chain. When it comes to comparison with a classic control loop, the following needs to be mentioned:

- The reference signal is the centre of the image. This is because the center of the acquired image is a straightforward estimation of the motor output position (and hence the telescope)
- The feedback signal (measured one) is the center of the Sun shape determined by the Sun tracking algorithm
- The error to be fed into controller is therefore a difference between the reference and the feedback signals — this translates into two channels (one for X and one for Y axis) — the controller can be a classic PI one
- Finally the controller output is translated into a pulse sequence suitable for stepper motors. The controller can be implemented in software.

The resulting control system is basic and robust, and together with the image processing system can function autonomously. It can be bypassed by the operator (control of which would be through the serial terminal) and it can take over if the operator is not connected to the system anymore. As an example, using a Raspberry PI for the board computer along with the PiCamera for the optical sensor, the feedback loop is illustrated in Figure 3.5.1.1.

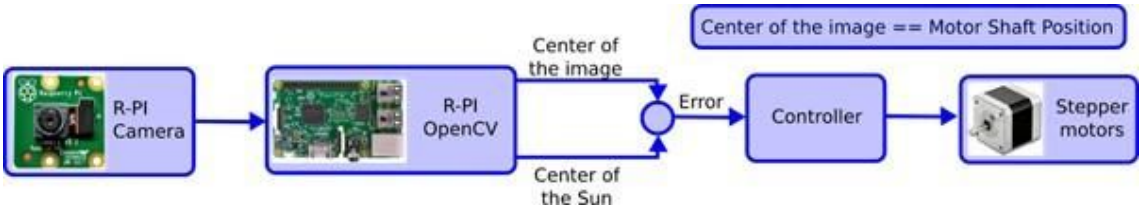

Figure 3.5.1.1. – Proposed control loop for actuation system.

The way the control system will work considering all elements is a two degree method in which first, the Sun estimation positioning from the 360 degree image will be applied followed by the Sun-tracking algorithm. Both stages are composed of two proportional-integral (PI) controllers, one per axis. For the first stage the magnitude of the error is directly calculated in degrees while for the second one, a conversion is made from pixels to degrees to calculate the deviation error from the centroid of the image.

In the case of the Sun-tracking algorithm, the pi-camera module has a resolution of 640x480 while the field of view in degrees is 62.2 for the horizontal and 48.8 for the vertical. That leaves approximately 0.0972 degrees per pixel or close to 350 arcseconds per pixel in the horizontal axis, and 0.1017 degrees per pixel (366 arcseconds) in the vertical axis. Given that, as explained at the Experiment Description section, The Sun, as perceived by an observer at the Earth, subtends an angle of approximately 0.52 degrees, it will cover around 5.35 and 5.11 pixels in the horizontal and vertical axis respectively. It is then possible to affirm that with more than 5 pixels the Sun-tracking algorithm will have the ability to align the telescope properly.

3.5.2. Power design

A power distribution unit is being studied during the construction of the latest version of this document. Our preliminary power consumption details are given in table 3.5.2.

Table 3.5.2.1. – Power System Breakdown

Element	Power (W)	Quantity	Total (W)
Arduino	0.4	3	1.2
Raspberry PI	3.75 (max)	2	7.5
Camera	1	3	3.0
Stepper Motor	7.00	2	14.0
Motor	1.00	1	1.0
Etalon Heating System	15 (max)	1	15.0
DC/DC Converters	6.0 (90% eff)	1	4.2
Total	-	-	45.87W*

**Note, this is the peak expected power, this is not expected to be required most of the time of the flight.*

Values provided in the power table are rated values. It is now known from experience that the real power consumption is below those values which points out to the possibility of relying in the power management strategy described in this document.

The telescope actuation and image processing system consists of several components with the electrical power consumption roughly equally distributed among them. The system assumes a single entry point coming from the balloon's batteries — from there the electrical power is brought to the parameters required by various components using DC-DC converters as it follows:

- 1 converter 30/5 V for Arduino, Raspberry Pi, cameras and sensors,
- 1 converter 30/24 V for motors

The DC/DC converters number is kept down by connecting multiple components in parallel if they share the same voltage parameters.

3.6. Software design

In this section, the software architecture as well as its supporting hardware are discussed. The hardware is only mentioned at an elevated level and only brought into view particularly if it has some limiting characteristics which needs to be circumvented. The software design concerns several directions:

- Sun tracking
- image processing
- image focusing
- diagnostics and monitoring
- start sequence and in-flight development
- energy management
- stepper motor control strategy
- redundant systems
- ground systems/telemetry

To successfully complete the experiment, a minimal setup consisting only of the Sun tracking and image processing needs to be present and able to function in fully autonomous manner. Given the challenging environmental conditions and the fact that physical access to the experimental setup during the flight is impossible, some redundancy as well as monitoring (through telemetry) should be implemented. This in turn requires the presence of the ground station systems which will allow manual (i.e. operator based) intervention using telemetry as well as in-flight data collection. To organize various components and make them communicate with the ground station for monitoring and diagnostics purposes, a local network is implemented using an industrial network switch. Whenever possible, the versions for controllers or computer boards used will be chosen in order to have an Ethernet port to connect to the network switch. The energy management section is required to efficiently use the available battery resources and redirect spare power towards heating (or heat loss compensation) of the critical components of the system (i.e. telescope). The start sequence details the system boot sequence (order of various controllers, PC, etc. to come online). Finally, the stepper motor control strategy is going to be detailed. The directions are going to be detailed next.

3.6.1. Overall View of the Software/Hardware Architecture

In this section, the software and underlying hardware architecture are presented. A general overview of the system is given as well as the relations between various components. Figure 4.59 illustrates the hardware architecture that is to be used.

The components listing, their role in the system, as well as the way they are implemented is provided below:

- Main controller (mission controller) - this component is the entry point of the system. It controls the rest of the components, being critical therefore a secondary controller is added (for redundancy). It communicates with the ground station the monitored data of the entire system. It keeps track of the rest of the components, making sure the proper ones are online when required, does the energy management, etc. For example it starts the computers when a certain altitude has been reached (or a certain time amount has passed since launching, or the ground operator has issued the command). It is equipped with relays so for example if the aquisition computer crashes, it can reboot it. A EtherMega is used to implement this controller - this is an Arduino with Ethernet port, 4 available relays and PCB mounts for its pins which

makes it a compact solution as well as provides more reliable connections with the rest of the system;

- Scientific acquisition system, Raspberry Pi and CCD sensor. Images are acquired using OpenCV in Python
- Positioning Controller - this controller interfaces between the Raspberry Pi unit and motors and is implemented using an EtherMega microcontroller which is Arduino Mega 2560 compatible having an Ethernet port as well. The Ethernet port allows manual positioning (i.e. by a ground operator). Also, a high number of pins are available in order to accommodate the motor requirements;
- Focusing Controller. This controls the motor for focusing the camera. An Arduino EtherMega is used for that purpose;
- Raspberry Pi with logic for Sun tracking;
- Controllers for various sensors (altitude, temperature, etc.) These are implemented using Arduino Nanos;

3.6.2. Sun tracking system

The *tracking* system is divided into two parts; the high-speed tracking and the fine adjustment tracking system. This functionality refers to both location and correction of the telescope position until the Sun's center coincide with the camera center. The tracking is split into two parts:

- first stage tracking going on at high speed but lower accuracy using either full or half-step control for the stepper motors. The telescope initial position is not important;
- second stage which does a more accurate positioning as well as detection and involves using micro-stepping control but is slower in speed. The telescope initial position will assume that the Sun disc is already contained in the tracking camera field of view due to the first stage completion.

The reason why there arises a need to perform tracking in two parts is because the visual tracking system is expensive in terms of computational resources as it requires using computer vision algorithms to process the video stream coming from the tracking camera. Furthermore, the current design of detection algorithm can only work once the Sun disc is entirely contained in the tracking camera field of view.

The first stage Sun tracking can be implemented using one of the following options:

- using look-up tables with astronomical data and input from sensors, GPS or compass;
- using photoresistors;
- using a 360°camera.

The look-up table solution starts from the idea that the Sun location is accurately known at each time of the year in advance. Using GPS and compass data, the local position and direction of the telescope with respect to the Sun can be determined easily and hence corrected. This is illustrated below, where the position of the Sun is calculated using spherical coordinates.

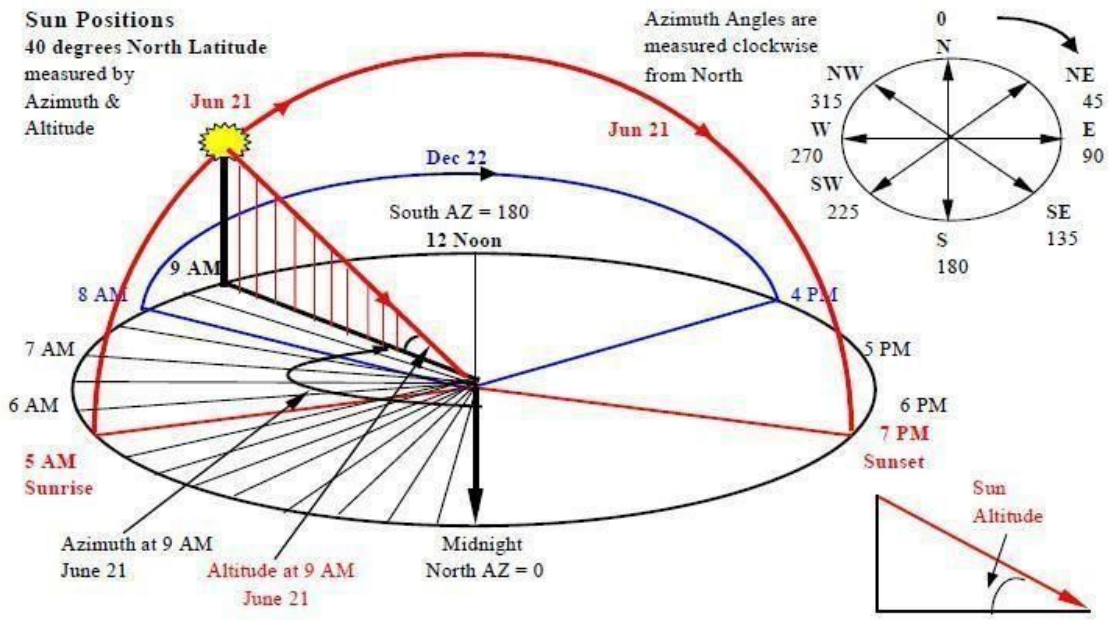

Figure 3.6.2.1. – Position of the Sun relative to a point on Earth at specific time in spherical coordinates.

As a proof of concept, using very simple hardware and a LabVIEW implementation, an experiment was conducted showing that the positioning error is within -/+ 2 degrees. This, along with its simplicity justifies this method and the team's preferences towards it. The experiment is described in Section 4.3.1. of the Appendix.

The photoresistors solution previously mentioned in the Electronics section assumes surrounding the gondola with a band of photoresistors which can give an indication based on the light they receive about the Sun position. This solution, while cheap and reliable will most likely not be necessary given the well-developed state of the primary solution, but it could allow for a small degree of coverage in case of software failure, especially given the possibility of implementation on a microcontroller in opposition to most software been developed in the Raspberry Pi. Some basic implementation is presented in "Appendix C - Electrical Testing".

The 360 degrees camera option would be implemented as a last resort if the previous two options don't lead to a satisfactory solution because it will require an image processing algorithm to establish the Sun's position as well as a preferential positioning on the gondola in order to avoid limiting its field of view.

The second stage implements a different Sun tracking algorithm and only kicks in when the first stage positioning has brought the Sun disc into the camera's field of view. At this stage, an actual detection of the Sun shape (and hence position) is going on based on OpenCV computer library operating on the video stream from the tracking camera.

In order to clearly distinguish between first and second stages we are going to refer to the first one as either the exploration phase or the actual Sun tracking phase while when it comes to the second one as detection or vision tracking stage (since it uses computer vision algorithms to detect the Sun position). A third phase would be required (capture the images) to ensure the experiment success. The details concerning each phase and how they work together are detailed next:

1. **Exploration Phase** The video signal acquired from the camera is continuously investigated until bright regions above a certain area (i.e. pixels with luminosity of range 230-255) from the image are detected. This assumes that the brightest object in

the image is the Sun. *In fact, detecting bright regions is a condition to ensure the success of the exploration phase and continue with the detection phase*. Once bright regions are detected, a vector is created that contains the Euclidean distance from the centre of the input image to the centre of the region of the brightest pixels. This idea is demonstrated below:

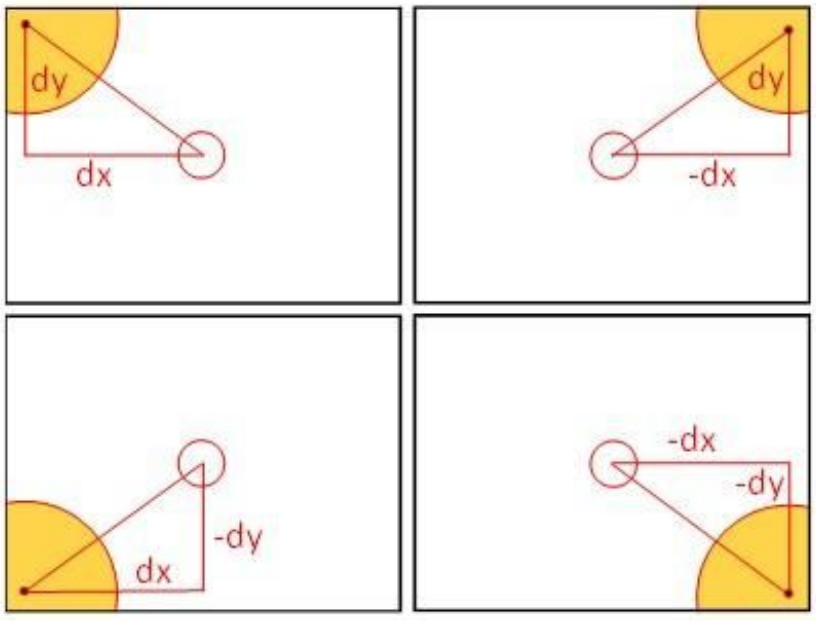

Figure 3.6.2.2 – Cases where the bright regions are detected with various possibilities.

Note this is NOT synonymous to tracking of the centroid of the Sun in phase 2, although the two methods have similar underlying methods, the purpose of this example is to align the telescope to the brightest section of the image

2. **Detection Phase** Once in line, the Phase 2 will begin by running a shape detection algorithm that will check to see if the captured bright image is a circle. Once detected it will then obtain its centroid and align it to the centre of the image. Therefore, this is similar with stage 2 mentioned above
3. **Capturing Phase** The final phase will result in signalling the computer handling the more expensive camera to start taking shots of the Sun and hence store in the memory storage as the telescope was aligned in the proper direction. The entire process can be visualized below.

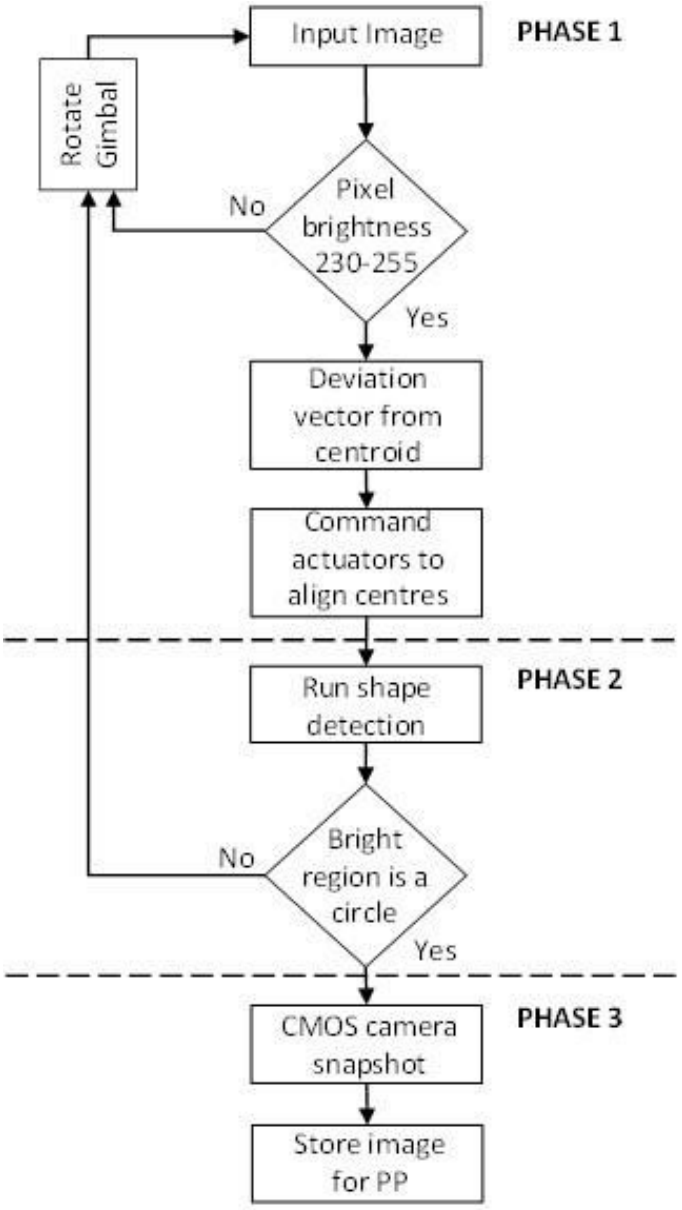

Figure 3.6.2.3. – Proposed design for the algorithm flowchart.

3.6.3. Monitoring and diagnostics

The monitoring capabilities assumes collecting data about various components and characteristics of the system and send them back to the ground station through the use of the E-link system. The bandwidth is going to be small as the data is going to consist mainly of text. The entire system is monitored by a microcontroller which collects the following parameters: • temperature on some key components prone to heating (like the motors or the image processing computer CPU) • "alive"signals from the Raspberry Pi as well as the computer handling the ZWO ASI120MM (mono) camera. These will be restarted if they don't generate the "alive" signal for a period of time (for instance 5 seconds)

The diagnostics are going to be performed if during the monitoring phase some sort of fault occurs. The diagnostic functionality can be split in two stages:

- during the prototype phase and pre-flight when extensive measurements are conducted (for example energy usage scenarios are tested to determine compliance with the available battery capacity)

- during the flight itself when only a very useful handful of diagnostics are collected

The possible actions available to the ground station operator are going to be taking control (manual mode) of the telescope positioning and focusing, restarting the on-board computers, etc.

3.6.4. Redundancy

Single focal point telescope accepts only one camera which requires in turn a performance computer. Due to constraints of telescope design, weight and power consumption, redundancy cannot be fully implemented for these two components. However, extra care is taken for auxiliary systems such as the monitoring or tracking one. Redundancy is partially implemented at the level of the tracking and monitoring systems. A secondary camera (PiCamera v2.1) and board computer (Raspberry Pi) are present for the tracking purposes. The monitoring microcontroller (Arduino like) is also doubled by another redundant one.

4. Post-Flight Activities

After the flight, the collected data will be downloaded for processing. However, since we aim to obtain scientific information from the time series of data, we intend to go beyond standard image processing, e.g., correcting intensity. For proper analysis of the plasma dynamics of the lower solar atmosphere we will have to remove the effects of e.g., solar rotation, spacecraft jitter and cosmic ray spikes, from the time series.

Although the first mission is planned for testing the proposed light-weight equipment, the obtained data will potentially have scientific value since the images will contain information on large-scale solar chromospheric activity, flows and oscillations measured with a very high time cadence. This information is much sought after in both the solar and stellar physics international communities. High-cadence full-disk, or Sun-as-a-star H-alpha observations will provide a connection between the integrated chromospheric intensity and the chromospheric activity, with potential applications to measurements of chromospheric activity of other stars. Furthermore, if a very high energy event takes place during the flight, e.g., a flare or coronal mass ejection, this will add even more scientific value to the obtained experimental data.

Additionally, we plan to compare data collected with data obtained by solar telescopes on the ground. For example superpositioning will enable us to determine the exact advantages of a balloon telescope system.

The high resolution solar images will also be used for outreach activities to promote Science and Engineering (see outreach section). From a more technical point of view, the proposed project will enable us to test the proposed stabilisation and observation system for using in the future missions. We anticipate that subsequent SunbYte telescopes shall become important and economically sustainable instruments of a high atmosphere- borne solar observatory. In the Figure 4.1 we have shown an example of images we expect to capture during SunbYte mission:

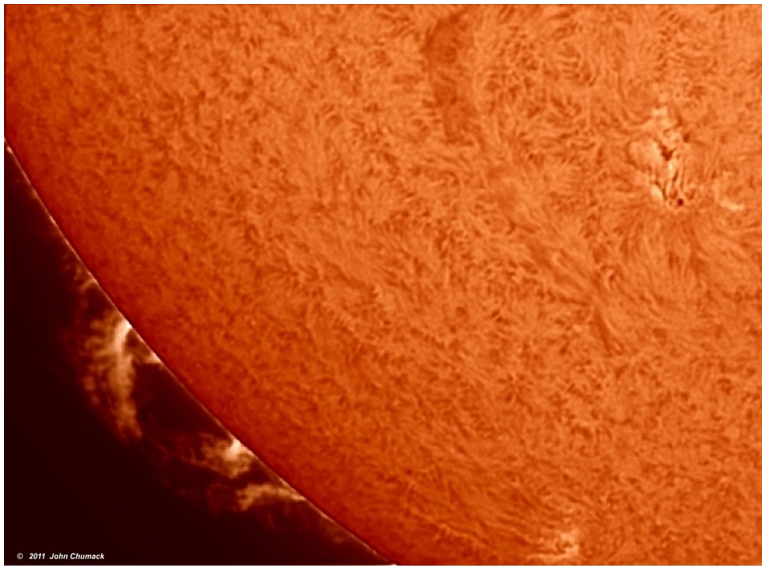

Figure 4.1 – Image of the Sun with an H-alpha filter, courtesy of John Chumack

5. Abbreviations and References

5.1. Abbreviations

Add abbreviations to the list below, as appropriate and delete unused abbreviations.

AIT	Assembly, Integration and Test
asap	as soon as possible
CDR	Critical Design Review
COG	Centre of Gravity
CRP	Campaign Requirement Plan
DLR	Deutsches Zentrum fA˜¼r Luft- und Raumfahrt
EIT	Electrical Interface Test
ESA	European Space Agency
Esrange	Esrange Space Center
ESTEC	European Space Research and Technology Centre, ESA (NL)
ESW	Experiment Selection Workshop
FAR	Flight Acceptance Review
FST	Flight Simulation Test
FRP	Flight Requirement Plan
FRR	Flight Readiness Review
GSE	Ground Support Equipment
H/W	Hardware
ICD	Interface Control Document
I/F	Interface
IPR	Integration Progress Review
LO	Lift Off
LT	Local Time
LOS	Line of Sight
Mbps	Mega Bits per second
MFH	Mission Flight Handbook
PCB	Printed Circuit Board (electronic card)
PDR	Preliminary Design Review
PST	Payload System Test
RBF	Remove Before Flight
SNSB	Swedish National Space Board
SODS	Start Of Data Storage
SOE	Start Of Experiment
S/W	Software
T	Time before and after launch noted with + or -
TBC	To be confirmed
TBD	To be determined
WBS	Work Breakdown Structure

5.2. References

[1] Obama, B., 2016 Executive Order: Coordinating efforts to prepare the nation space weather events, The White House.
https://obamawhitehouse.archives.gov/the-press-office/2016/10/13/executive-order-coordinating-efforts-prepare-nation-space-weather-events
[2] Guzik, G. T., 2017, HASP Student Payload Interface Manual
http://laspace.lsu.edu/hasp/documents/public/HASP_Interface_Manual_v21709.pdf

Useful guidance documents:

- European Cooperation for Space Standardization ECSS: Space Project Management, **Project Planning and Implementation**, ECSS- M-ST-10C Rev.1, 6 March 2009
- SSC Esrange: **Esrange Safety Manual**, REA00-E60 , 23 June 2010
- European Cooperation for Space Standardization ECSS: Space Engineering, **Technical Requirements Specification**, ECSS-E-ST-10- 06C, 6 March 2009
- European Cooperation for Space Standardization ECSS, Space Project Management, **Risk Management**, ECSS-M-ST-80C, 31 July 2008
- European Cooperation for Space Standardization ECSS: Space Engineering, **Verification**, ECSS-E-ST-10-02C, 6 March 2009
- Project Management Institute, **Practice Standard for Work Breakdown Structures - second Edition**, Project Management Institute, Pennsylvania, USA, 2006

HASP Student Payload Application for 2018 Appendix

The University of Sheffield
Sheffield University Nova Balloon Lifted Telescope

Contents

1. Experiment requirements and constraints

1.1. Functional Requirements

F1. The camera shall successfully track the Sun.
F2. The experiment shall image the Sun in the spectral line of 656.28nm (H-alpha).

1.2. Performance Requirements

P1. The gimbal system shall direct the telescope towards the Sun with an accuracy of at least 1 arc second.
P2. The precision of the telescope shall be within a value of 1 arc second.
P3. The Sun shall be imaged at a maximum rate of 40 fps.
P4. The experiment shall produce an output with a resolution of 1 arc sec at the vacuum wavelength of H-alpha line core - 656.28nm.
P5. The maximum current drawn shall not exceed 3.5A.
P6. The supporting structure shall withstand a maximum compressive load of 200 N.
P7. The tracking camera shall have a video resolution of no less than 640 by 480 pixels and 30 fps.

1.3. Design Requirements

D1. The experiment shall operate in the temperature profile of the HASP vehicle flight and launch.
D2. The experiment shall operate in the vibration profile of the HASP vehicle flight and launch.
D3. The experiment shall operate in the pressure profile of the HASP vehicle flight and launch.
D4. The experiment shall not disturb or harm the launch vehicle.
D5. The experiment shall not broadcast at a frequency prohibited in Texas.
D6. The diameter of the primary mirror shall not exceed 85 mm.
D7. The length of the telescope shall not exceed 380 mm.
D8. The mass of the experiment shall not exceed 20 kg.
D9. The maximum tolerance of any gearing has to be within 0.2 arcsec.
D10. The Sun sensor shall detect intensities of up to 100,000 lux.
D11. The supporting structure shall not twist by more than 0.1 degrees.
D12. The supporting beam shall not buckle under a safety factor of 2.
D13. The experiment shall be able to run for up to 20 hours.

1.4. Operational Requirements

O1. The experiment shall accept control of the focusing motor for manual focus if a command is sent.
O2. The experiment shall enter the searching pattern if the location of the Sun is not found according to the astronomical algorithm.
O3. The experiment shall transmit images to the ground when requested.
O4. The experiment shall cease to rotate on landing.
O5. The experiment shall be able to read data from a GPS device.

2. Verification

2.1. Verification Plan

In order to verify the requirements stated in section 1 of the appendix, the following verification table has been created.

Table 2.1.1. – Verification table

ID	Requirement text	Verification	Test No.	Status
F1	The camera shall successfully track the Sun.	T	**1, 2, 3**	**Achieved**
F2	The experiment shall image the Sun in the spectral line of 656.28nm (H-alpha).	T,R	**23**	**In Progress**
P1	The gimbal system shall direct the telescope towards the Sun with an accuracy of at least 1 arcsecond	T,R	**1, 2, 3, 23**	**In Progress**
P2	The precision of the telescope shall be within a value of 1 arcsec.	T,R	**4, 5, 23**	**In Progress**
P3	The Sun shall be imaged at a maximum rate of 40 fps.	T, R	**23, 26, 27**	**In Progress**
P4	The experiment shall produce an output with a resolution of 1 arcsec at the vacuum wavelength of H-alpha line core - 656.28nm.	T, R	**6, 7, 23, 26, 27**	**In Progress**
P5	The maximum current drawn shall not exceed 3.5A.	T	**8, 9**	**Achieved**
P6	The supporting structure shall withstand a maximum compressive load of 200 N.	T, A	**11**	**In Progress**
P7	The tracking camera shall have a video resolution of no less than 640 by 480 pixels and 30 fps.	T, R	**3, 26, 27**	**Achieved**

ID	Requirement text	Verification	Test No.	Status
D1	The experiment shall operate in the temperature profile of the HASP vehicle flight and launch.	T, A, R	**19, 22**	**In Progress**
D2	The experiment shall operate in the vibration profile of the HASP vehicle flight and launch.	T, A	**12**	**In Progress**
D3	The experiment shall operate in the pressure profile of the HASP vehicle flight and launch.	T, A	**24**	**Achieved**

D4	The experiment shall not disturb or harm the launch vehicle.	I, R	-	**Not completed**
D5	The experiment shall not transmit on frequencies prohibited in Sweden.	R	-	**N/A**
D6	The diameter of the primary mirror shall not exceed 200 mm.	R	-	**Achieved**
D7	The length of the telescope shall not exceed 1000 mm.	R	-	**Achieved**
D8	The mass of the experiment shall not exceed 25 kg.	R	-	**Achieved**
D9	The maximum tolerance of any gearing has to be within 0.2 arcsec.	T, R	**10, 13**	**In Progress**
D10	The Sun tracking camera shall detect intensities of up to 100,000 lux.	T, R	**3**	**Achieved**
D11	The supporting structure shall not twist by more than 0.1 degrees.	T, A	**11**	**In Progress**
D12	The supporting beam shall not buckle under a safety factor of 2.	T, A	**11**	**In Progress**
D13	The experiment shall be able to run for up to 3 hours.	T	**23, 24**	**In Progress**

ID	**Requirement text**	**Verification**	**Test No.**	**Status**
O1	The experiment shall accept control of the focusing motor for manual focus if a command is sent.	T	**21, 23. 26, 27**	**In Progress**
O2	The experiment shall enter the searching pattern if location of the Sun is not found according to the astronomical algorithm.	T	**15, 17, 26, 27**	**Achieved**
O3	The experiment shall transmit images to the ground when requested.	T	**21, 22**	**In Progress**
O4	The experiment shall cease to rotate on landing.	T	-	-
O5	The experiment shall be able to read data from a GPS device.	T	**25**	**Achieved**

2.2. Test Plan

Tests to be conducted in accordance to the verification table.

Table 2.2.1. – Test description

Test number	1
Test type	Software
Test facility	University of Sheffield
Tested item	Raspberry Pi tracking system
Test level/procedure and duration	This test was performed on a prototype of the Sun in the form a tennis ball. The idea was to gain confidence in the tracking abilities of the algorithm. The tennis ball was made to move in various positions and the distance from the centre of the screen and the center of the ball was recorded in two bits of data constituting the horizontal deflection cX and vertical deflection cY
Test campaign duration	1 hour
Test campaign date	8 March 2017
Test completed	Yes

Table 2.2.2. – Test description

Test number	2
Test type	Software
Test facility	University of Sheffield
Tested item	Raspberry Pi tracking
Test level/procedure and duration	This experiment was performed similar to P1 except it was repeated on a data set obtained from a camera with solar filter from one of the software team members (Alex Ian Hamilton).
Test campaign duration	6 hours
Test campaign date	15 March 2017
Test completed	Yes

Table 2.2.3. – Test description

Test number	3
Test type	Software
Test facility	University of Sheffield
Tested item	Raspberry Pi tracking
Test level/procedure and duration	The experiment was made to test the Sun visual tracking system in real time and was tested from the Raspberry Pi. The light source was taken to be a camera light from a cell phone. The purpose for this experiment was to test the performance of Raspberry Pi system).
Test campaign duration	3 hours
Test campaign date	17 March 2017
Test completed	Yes

Table 2.2.4. – Test description

Test number	4
Test type	Electrical
Test facility	University of Sheffield
Tested item	Arduino + Stepper motors
Test level/procedure and duration	The experiment was made to test control of at least two stepper motors with Arduino using as well the gimbal prototype for closest resemblance to final experiment. This would allow for two axis rotation of the telescope when tracking the Sun.
Test campaign duration	15 minutes
Test campaign date	17 March 2017
Test completed	Yes

Table 2.2.5. – Test description

Test number	5
Test type	Electrical
Test facility	University of Sheffield
Tested item	Arduino + Stepper motors
Test level/procedure and duration	Similar to test P4 but receiving the command values for rotation directly from the computer through serial communication. This test is crucial in order to set a connection between the hardware involved in Sun tracking and the Arduino which rules over the stepper motors.
Test campaign duration	15 minutes
Test campaign date	17 March 2017
Test completed	Yes

Table 2.2.6.

Test number	6
Test type	Software
Test facility	University of Sheffield
Tested item	PC Unit + Linux distribution + Andor SDK-based program + Andor camera
Test level/procedure and duration	Integrate and assess performance (fps, power consumption) of the data acquisition chain.
Test campaign duration	8 hours
Test campaign date	4 June 2017
Test completed	Yes

Table 2.2.7. – Test description

Test number	7
Test type	Software
Test facility	University of Sheffield
Tested item	Andor SDK
Test level/procedure and duration	Test and assess the Andor SDK for the features required by experiment by implementing various programs.
Test campaign duration	45 minutes
Test campaign date	28 April 2017
Test completed	Yes

Table 2.2.8. – Test description

Test number	8
Test type	Electrical
Test facility	University of Sheffield
Tested item	Raspberry Pi unit + Telescope camera (power consumption)
Test level/procedure and duration	Tested PC unit power consumption when operating Andor SCMOS camera under load using wattmeters.
Test campaign duration	45 minutes
Test campaign date	10 March 2018
Test completed	Yes

Table 2.2.9. - Test description

Test number	9
Test type	Electrical
Test facility	University of Sheffield
Tested item	DC/DC converters
Test level/procedure and duration	Test and assess performance and power losses of DC/DC converters under load operation (efficiency).
Test campaign duration	45 minutes
Test campaign date	14 May 2017
Test completed	Yes

Table 2.2.10. – Test description

Test number	10
Test type	Mechanical
Test facility	University of Sheffield
Tested item	Harmonic Drive
Test level/procedure and duration	Test harmonic drive.
Test campaign duration	1 day
Test campaign date	8 Aug 2017
Test completed	Yes

Table 2.2.11. - Test description

Test number	11
Test type	Mechanical
Test facility	University of Sheffield
Tested item	Gimbal Support Structure
Test level/procedure and duration	Load supporting structure 200N in compression for 3 hours.
Test campaign duration	3 hours
Test campaign date	15 August 2017
Test completed	Yes

Table 2.2.12. - Test description

Test number	12
Test type	Mechanical
Test facility	Sheffield
Tested item	Full Structure Assembly
Test level/procedure and duration	Vibrations test. Secure experiment in a van and drive on bumpy road.
Test campaign duration	3 hours
Test campaign date	12 September 2017
Test completed	No

Table 2.2.13. – Test description

Test number	13
Test type	Software
Test facility	University of Sheffield
Tested item	stepper motor control strategy
Test level/procedure and duration	The stepper motors will be tested with a microstepping driver for issues like accuracy, speed response, etc.
Test campaign duration	8 hours
Test campaign date	15 August 2017
Test completed	Yes

Table 2.2.14. – Test description

Test number	14
Test type	Electrical/Software
Test facility	University of Sheffield
Tested item	360 degrees camera + Raspberry-Pi + OpenCV
Test level/procedure and duration	Test feasibility of a 360 degree camera coupled with Raspberry-Pi for stage 1 Sun tracking method
Test campaign duration	3 hours
Test campaign date	24 Jan 2018
Test completed	No

Table 2.2.15.

Test number	15
Test type	Electrical/Software
Test facility	University of Sheffield
Tested item	Compass sensor + Arduino + Motor + LabVIEW
Test level/procedure and duration	Test feasibility of stage 1 Sun tracking method based on magnetic compass sensor and astronomical data.
Test campaign duration	8 hours
Test campaign date	06 Feb 2018
Test completed	No

Table 2.2.16. – Test description

Test number	16
Test type	Electrical/Software
Test facility	University of Sheffield
Tested item	Photoresistors + Arduino
Test level/procedure and duration	Test feasibility of a stage 1 Sun tracking method based on photoresistor array.
Test campaign duration	2 hours
Test campaign date	10 March 2018
Test completed	No

Table 2.2.17. – Test description

Test number	17
Test type	Electrical/Software
Test facility	University of Sheffield
Tested item	Sun tracking integration of stages 1 and 2
Test level/procedure and duration	Integrate the track algorithms. The main components involved in the test are the Raspberry pi and the EtherMega.
Test campaign duration	2 hours
Test campaign date	20 March 2018
Test completed	No

Table 2.18. – Test description

Test number	18
Test type	Electrical
Test facility	University of Sheffield
Tested item	DC/DC converter, driver, stepper motor and Arduino
Test level/procedure and duration	Level of noise measured with an oscilloscope in various points during working conditions.
Test campaign duration	45 minutes
Test campaign date	30 April 2017
Test completed	Yes

Table 2.19. – Test description

Test number	19
Test type	Electrical/Thermal
Test facility	University of Sheffield
Tested item	Stepper motor
Test level/procedure and duration	Assess the ability of the stepper motor and sensors to withstand low temperature.
Test campaign duration	4 hours
Test campaign date	5 September 2017
Test completed	Yes

Table 2.20. – Test description

Test number	20
Test type	Software
Test facility	University of Sheffield
Tested item	Ether Mega operational test and integrated system response
Test level/procedure and duration	Test the main controller communication with other components and the system response (i.e. the speed with which the PC unit, camera, etc. come online after shutdown)
Test campaign duration	4 hours
Test campaign date	10 June 2017
Test completed	Yes

Table 2.21. – Test description

Test number	21
Test type	Software
Test facility	University of Sheffield
Tested item	Energy management (entire system)
Test level/procedure and duration	Test and tweak the energy consumption (test performed mainly at the main controller level)
Test campaign duration	4 hours
Test campaign date	12 June 2017
Test completed	Yes

Table 2.22. – Test description

Test number	22
Test type	Electrical/Software/Thermal
Test facility	Manufacturer facility
Tested item	Heating the telescope (entire system)
Test level/procedure and duration	This test is performed by the manufacturer and the results provided to us
Test campaign duration	4 hours
Test campaign date	1 June 2017
Test completed	Yes

Table 2.23. – Test description

Test number	23
Test type	Integration
Test facility	University of Sheffield
Tested item	Full Assembly
Test level/procedure and duration	Test integration with telescope positioning system.
Test campaign duration	20-30 hours
Test campaign date	12 September 2017
Test completed	No

Table 2.24. – Test description

Test number	24
Test type	Electrical
Test facility	Northumbria University
Tested item	Actuator and all electronics
Test level/procedure and duration	Test actuator and electronics in vacuum chamber for 2 hours.
Test campaign duration	2 days
Test campaign date	21 August 2017
Test completed	Yes

Table 2.25. – Test description

Test number	25
Test type	Electrical
Test facility	University of Sheffield
Tested item	Magnetic compass sensor readings
Test level/procedure and duration	Test accuracy of magnetic compass sensor readings.
Test campaign duration	2 hours
Test campaign date	1 August 2017
Test completed	Yes

Table 2.26. – Test description

Test number	26
Test type	Electrical/Soft
Test facility	University of Sheffield
Tested item	Thermocouples
Test level/procedure and duration	Test the accuracy of the thermocouples for reading the temperature of the actuators in operation.
Test campaign duration	1 hour
Test campaign date	18 August 2017
Test completed	Yes

Table 2.27. – Test description

Test number	27
Test type	Electrical/Soft
Test facility	University of Sheffield
Tested item	Electronics
Test level/procedure and duration	Preparte electronics setting including motor under operation for vacuum testing at Northumbria University.
Test campaign duration	2 days
Test campaign date	20 August 2017
Test completed	Yes

2.3. Test results

Table 2.3.1

Test	Outcome	Obtained Results
F1	Success	The camera successfully tracked the Sun
F2	Pending	-
P1	Pending	Raspberry-Pi performs adequately
P2	Pending	-
P3	Pending	-
P4	Pending	-
P5	Success	A limit on the withdrawal of current beyond 3.5A achieved
P6	Pending	-
P7	Success	The sun sensor successfully detected intensities up to 100,000 lux
D1	Pending	-
D2	Pending	-
D3	Success	The actuator and electronics performed successfully in a vacuum chamber for 2 hours.
D9	Pending	-
D10	Partial Success	The camera successfully tracked the object indoors. More testing to be done outdoors
D11	Failed	Brackets to be manufactured to prevent twisting.
D12	Pending	-
D13	Pending	-
O1	Pending	-
O2	Partial Success	Successful Tests: 15, 17, 26 Test 27: Most elements where fully functional except for the ethernet switch, pi camera (on but not under operation) and current sensors (on but now logging data)
O3	Pending	-
O4	Pending	-
O5	Partial Success	The magnetic compass is highly affected by PMs, solved by moving sensors into gimbal structure.

3. Cost

3.1. Expenditure

3.1.1. Electronics

Payload Materials	Cost(£)	Quantity	Total(£)	Total(e)
Electrical				**1.13**
Actuators	30.00	6	180.00	203.40
IMU	40.00	3	120.00	135.60
Cable (RPi->arduino)	4.00	1	4.00	4.52
Raspberry Pi 3 Model B	34.00	2	68.00	76.84
Motor Drivers	25.00	6	150.00	169.50
USB Imager	200.00	1	200.00	226.00
Pi camera cable	2.50	1	2.50	2.83
Various DC-DC converters (28V-12V, 5V-12V)	12.00	2	24.00	27.12
64GB MicroSD card	20.00	2	40.00	45.20
Dupont wires	6.00	1	6.00	6.78
EtherMega (Arduino like)	89.00	3	267.00	301.71
Stepper motors 0.36 degs/step + driver + cable	109.00	1	109.00	123.17
Raspberry Pi Heat sinks	4.00	2	8.00	9.04
Raspberry Pi Camera Mount	6.00	2	12.00	13.56
Power Supply (Variable 0-30V, 0-5V)	74.00	1	74.00	83.62
Power Meters	14.00	3	42.00	47.46
Micro USB Cables (Arduino)	1.00	3	3.00	3.39
Micro USB Power Connector (Raspberry Pi)	1.70	1	1.70	1.92
Amphenol RJF21B	21.95	1	21.95	24.80
Amphenol MS3112E8-4P	7.45	4	29.80	33.67
Amphenol 62GB Series, 41 weight box mount MIL Spec circular connector receptacle, socket contacts, shell size 20	37.81	1	37.81	42.73
Amphenol 62GB Series, 41 weight box mount MIL Spec circular connector plug, pin contacts, shell	48.00	1	48.00	54.24

size 20				
D-sub 9 way connector plug	9.00	2	18.00	20.34
D-sub 9 way connector socket	9.00	2	18.00	20.34
D-sub 25 way connector plug	26.44	1	26.44	29.88
D-sub 25 way connector socket	28.00	1	28.00	31.64
Thermocouple Amps	21.37	6	128.22	144.89
Thermocouple	17.17	6	103.02	116.41
Logic Level Shifter	9.00	2	18.00	20.34
PCB USB A connectors	0.63	10	6.30	7.12
PCB micro USB A connectors	0.53	2	1.06	1.20
50 Pcs Brass Screw Thread PCB Stand-off Spacer	5.43	1	5.43	6.14
		Totals:	**1801.23**	**2035.39**

3.1.2. Mechanical

Payload Materials	Cost(£)	Quantity	Total(£)	Total(e)
Mechanical				**1.13**
Aluminium 6082 tubing	200	1	200.00	226.00
PLA/ABS filament	30	2	60.00	67.80
Harmonic Drives - HFUC - 2UH	925	2	1850.00	2090.50
Low temperatures performance grease: ZFE-60ml-Flexolub-M0	107	60ml	107.00	123.05
Aluminium Box Tube - 1” Square x 16swg x 1000mm Long	5.39	1	5.39	6.09
Aluminium Box Tube - 40mm Square x 2.5mm Wall x 1000mm Long	10.48	1	10.48	11.84
Aluminium Box Tube - 1” Square x 16swg x 750mm Long	4.57	1	4.57	5.16
Aluminium Box Tube - 40mm Square x 2.5mm Wall x 500mm Long	6.2	1	6.20	7.01
Aluminium 6082 Square Tube - Square x 16swg x 1000mm Long	5.7	1	5.70	6.44
Aluminium Square Tube - 1” Square x 16swg x 750mm Long	4.82	1	4.82	5.45
Aluminium Square Tube - 40mm Square x 2.5mm Wall x 1000mm Long	11.07	1	11.07	12.51
Aluminium Square Tube - 40mm Square x 2.5mm Wall x 500mm Long	6.55	1	6.55	7.40
Aluminium Square Tube - in Square x 16swg x 2500 Long	8.57	1	8.57	9.68
Aluminium Square Tube: 1” Square x 16swg x 750mm Long	4.57	2	9.14	10.33
Aluminium Box Tube - 19.05 Square x 1.6 Wall x 1000mm	4	3	12.00	13.56
Aluminium Box Tube - 25.4 Square x 1.6 Wall x 1000mm	4.9	2	9.80	11.07
Aluminium 6082 Plate - 200 square x 1.5mm	10	1	10.00	11.30
Aluminium 6082 Plate - 160 x 180 x 2.5mm	6	1	6.00	6.78
Aluminium 6082 Plate - 110 x 100 x 2.5mm	4	1	4.00	4.52
Aluminium 6082 Plate - 750 x 170 x 2.5mm	24	1	24.00	27.12
Aluminium 6082 Plate - 760 x 100 x 2.5mm	20	1	20.00	22.60
Aluminium 6082 Plate - 1500 x 750 x 2.5mm	49	2	98.00	110.74
Aluminium 6082 Plate - 330 x 300 x 2.5mm	7	2	14.00	15.82

Aluminium 6082 Plate - 200 x 300 x 2.5mm	6	2	12.00	13.56
Aluminium 6082 Plate - 350 x 180 x 2.5mm	6	2	12.00	13.56
Aluminium 6082 Plate - 210 x 300 x 2.5mm	6	2	12.00	13.56
C7109 Aluminized Mylar Film	39.72	2 metres	39.72	45,28
Bearings 6900-2RS	10.8	1	10.80	12.20
Aluminium Round Bar - 2” Diam x 100mm Long	10.91	1	10.91	12.33
Steel plate 25 x 25cm	21	1	21.00	23.73
Loctite (40ml)	43	1	43.00	48.59
DIN rail	14	1	14.00	15.82
Aluminium Angle - 3” x 1 1/2 ” x 1/8” x 1000mm Long	8.96	1	8.96	10.12
Aluminium Angle - 3” x 1 1/2 ” x 1/8 ” x 500mm Long	6.02	1	6.02	6.80
Draper 12-Piece 140 mm Needle File Set	8.5	2	17.00	19.21
19mm Wide High Temperature Kapton Polyimide Tape	7.03	1	7.03	7.94
		Totals:	**#VALUE!**	**2887.16**

3.1.3. Optics

Payload Materials	Cost(£)	Quantity	Total(£)	Total(e)
Optics				**1.13**
Meade ETX 125 Telescope	700.00	1	700.00	791.00
Solar Filter	100	1	100.00	113.00
Modifications (lighten, degrease, etc.)	200	1	200.00	226.00
0.4x Telecentric	249	1	249.00	281.37
Research grade etalon - 0.50 Angstrom	6,510.83	1	6510.83	7357.24
		Totals:	**7759.83**	**8768.61**

3.2. Income

Table 3.1. – Funding

Source Funding	**Amount(GBP)**	**Amount (USD)**
ACSE (Sheffield University)	4,400	5,896
Northumbria University	2,000	2,680
Widening Participation from Faculty of Engineering (Sheffield University)	5,000	6,700
Sheffield Festival of Science And Engineering	35	47
Sheffield Engineering Leadership Academy	1,000	1,340
Andor company	12,000	16,080
University of Sheffield SURE program for students to work on project	6,480	8,683
Public Engagement Competition	500	670
UKSEDS	400	536
School of Mathematics and Statistics	4,000	5,360
Alumni Fund	6,000	8,040
Total	41,815	56,032

4. Additional Technical Information

4.1. Mechanical

4.1.1. General assembly drawings

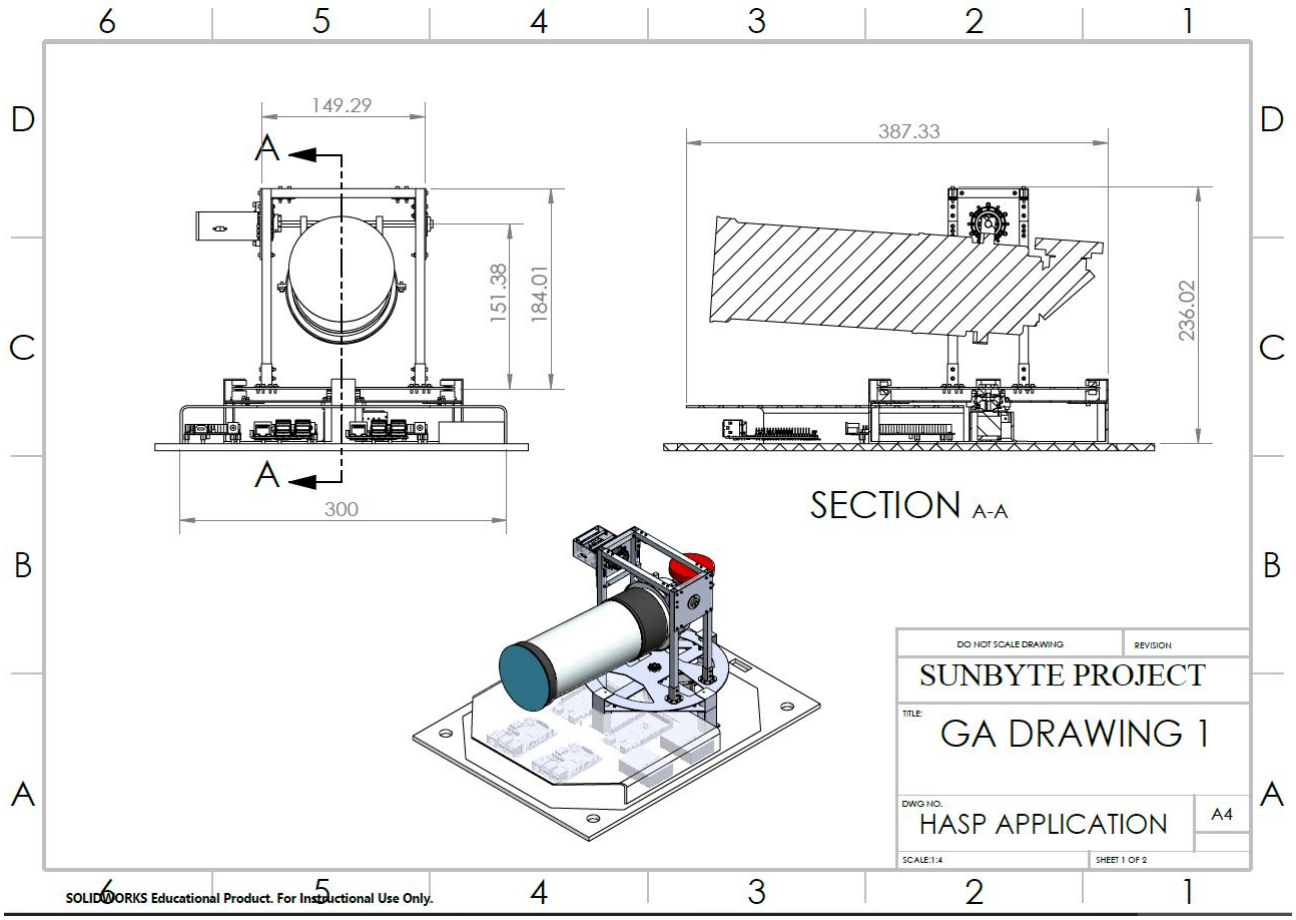

Figure 4.1.1.1. – General Assembly Drawing, page 1

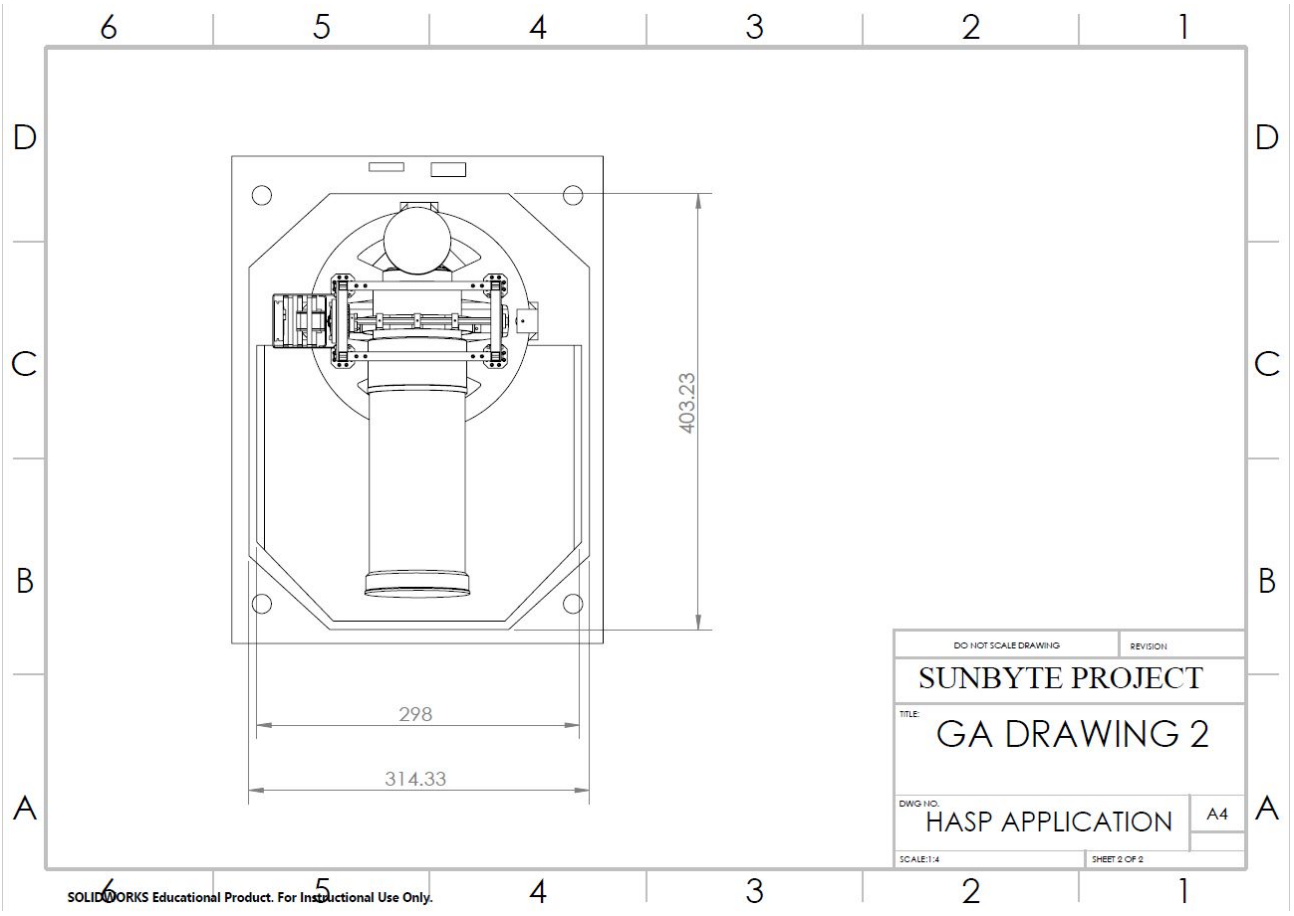

Figure 4.1.1.2. – General Assembly drawing, page 2.

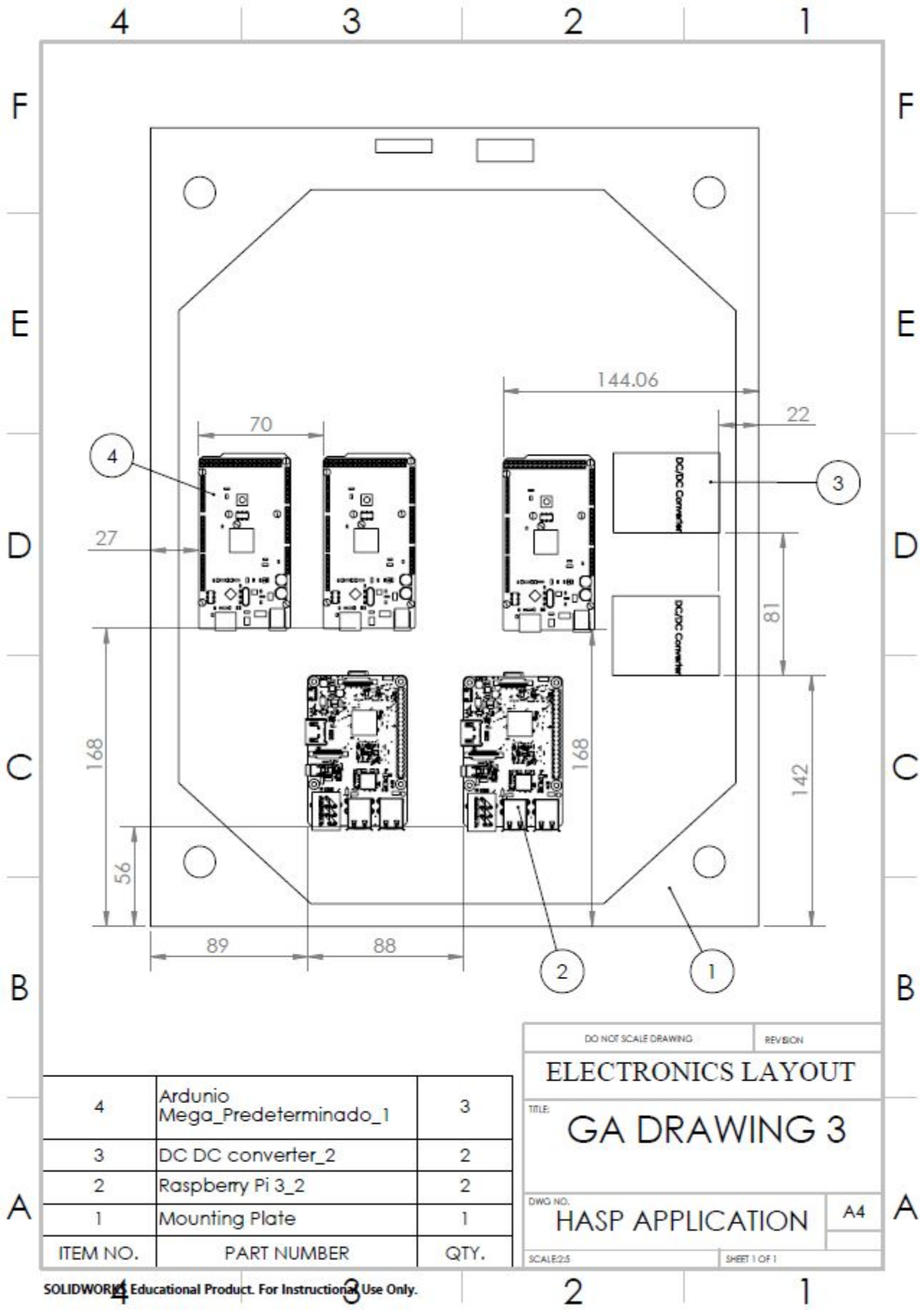

Figure 4.1.1.3. – General Assembly drawing, page 3.

4.1.2. Material Selection for the Gimbal and Support Structure

The possible materials that can be used for the gimbal are shown below in the table on the next page. The Yield strength of the materials has been taken over the expected temperature range to which the gimbal will be exposed to (approx -80 °C to 30 °C). The programme used to gather the data was CES Edupack 2016. Table 4.4 is a decision matrix used in order to choose the material we are most likely to use. Reliability was chosen to be the most important because at 25 km in the air, it would be impossible to change or fix any parts so they need to work as well in the air as they do on the ground. Only three of the materials have been shown as they are the most likely to be used for the gimbal. Using this matrix, Aluminium has the highest and most consistent scoring of the materials. Aluminium is also more readily available, easily extrudable and will still show some ductility at the approximate temperature ranges. It is difficult to 3D print the aluminium, so a different manufacturing process should also be considered. A key material property considered in the initial design selection process was the ability of the material to be 3D printed. However, after further testing a 3D printed model has been implemented. Further testing will be considered shortly and if the model survives the vacuum chamber test that is to be conducted, we might reconsider the possibility of using the aluminium model. At the moment, the possibility of using 3D printing as the main manufacturing route has to be confirmed by testing.

3D printing metal for the current design is considered. If this method of manufacturing proves itself efficient and compatible with our mission we might consider using those components in the actual experiment assembly.

Table 4.1.1 - Material selection

Material	Strengths	Weaknesses	Yield Strength (MPa)	Density (kg/m^3)	Cost (£/kg)	Cost (€/kg)	3D printable	Solutions to weakness
ABS (40% carbon fibre)	Low density	Poor durabilityin UVradiation.	124- 131	1220-1270	6.78-8.77	7,70-9,97	Yes	Use of some type of coating against UV
Austenitic Steel 304	-Excellent corrosion resistance against water	-Heavy -3D printing questionable	190-310	7900	3	3,41	Yes-not very common	Machining each of the parts
Aluminium 6061	-High strength - widely used in Aerospace applications -High corrosion resistance -Easily machined -Easily weldable	-Not as lightweight as other options -Not as strong as Kevlar	241-266	2700-2730	1.57-1.8	1,78-2,25	Yes	The size of the gimbal is not very big; so the weight will not affect the total structure too much
Nylon 12 (with Aculon coating)	-Lightweight -Low water absorption -Good weather resistance	-Very low yield strength -Mechanical properties affected by moisture	34.8-43.4	1000-1020	7.16-8.7	8,14-9,89	Yes	Application of a coating to prevent moisture and UV
Kevlar (with coating)	-Tough, strong, impact resistant -Low coefficient of friction -Lightweight	-Affected by UV radiation -Mechanical properties affected by moisture	2500-3000	1460-1480	62.8-157	71,36-178,41	Yes	Application of a coating to prevent moisture and UV

Table 4.1.2 - Material comparison

	Kevlar	**Austenitic Steel 304**	**Aluminium 6061**
Weight (5)	3	1	2
Reliability (6)	1	3	2
Machinability (2)	1	2	3
Price Effectiveness (1)	1	2	3
3D Printability (1)	3	1	2
Corrosion Resistance (4)	1	2	3
Total score	37	40	49

Further material selection analysis has been conducted in order to decide upon the most suitable and compatible material to be used in the manufacturing processes. In conclusion, it has been decided that Aluminium 6082 would be the most suited material for both the gondola and the gimbal. The next step was getting in contact with potential suppliers and manufacturers. The final choice of the material was made between Austenitic Stainless Steel and Aluminium 6082. As the steel weighs approximately 3 times as much as the Aluminium. Therefore it was not a viable option as we need to put as little strain on the motors as possible to reduce that heat generation. AirCraftMaterials UK were contacted about having test samples made. One quote that we received for 10 samples to be used in various testing conditions was £420.

Table 4.1.3 - Material properties

	Austenitic Steel 304LN	**Aluminium 6082**
Service Temperatures (deg C)	-250 - 750	-273 - 150
Thermal Conductivity (W/m*K)	14.4 - 15.6	164 - 170
Specific Heat Capacity (J/kg*K)	500	882 - 918
Thermal Expansions Coefficient (micro strain/K)	16.5 - 17.5	22.5 - 23.7
Durability	Excellent	Excellent
Density (kg/m^3)	7900	2670 - 2730
Young's Modulus (GPa)	195 - 205	70 - 74
Yield Strength (MPa)	270 - 290	162 - 179
Tensile Strength (MPa)	550 - 750	247 - 273
Compressive Strength (MPa)	270 - 290	162 - 179

4.1.3. Torque and Gearbox Ratio Sizing

Assuming the gearbox shaft is mounted at the telescope's mass centre the motor will only have to provide friction compensation and acceleration torque. In determining the following, the largest perturbance known which is a 5 rpm spin during the ascent is used to size up the motors. The motor need to compensate the 5 rpm spin by accelerating in a reasonable amount (for example 0.1 s) then keeping the compensating speed at roughly 5 rpm (30°/s. Therefore, the worst-case scenario would be to accelerate from 0 to 5 rpm in 0.1 seconds:

$$\epsilon = \frac{30°/\mathrm{s}}{0.1\ \mathrm{s}} = 300°/\mathrm{s}^2 \tag{4.3}$$

The acceleration torque required is:

$$T_{dyn} = J * \epsilon = 1.4\ \mathrm{kg} * \mathrm{m}^2 * 300°/\mathrm{s}^2 * \pi/180 = 7.86\ \mathrm{Nm} \tag{4.4}$$

The inertia moment was computed for a rod with the mass of 18 kg uniformly distributed over a length of 1 meter which has an horizontal orientation but spins around a vertical axis of rotation, positioned in its mass centre. In reality this quantity (J) needs to be accurately determined from CAD or FE models. The 18kg figure is double the amount required, however, there are some unknowns, like the friction losses at low temperature, so it is adopted to cover those situation too. Introducing the gearbox (with a reduction factor n and efficiency ηG) the motor parameters are

$$T_{mot} = T_{dyn}/n/\eta_G \tag{4.5}$$

$$\Omega_{mot} = n * \Omega_G \tag{4.6}$$

$$P_{mot} = T_{dyn} * \Omega_G/\eta_G \tag{4.7}$$

If we consider a 5-phase stepper motor with a resolution of 0.36°/step, the possibility of microstepping up to the 1/20 and the requirement of 0.5 arcseconds, the reduction factor n of the gearbox is given by $n = 0.36/(1/7200)*1/20 = 130$. Therefore, the motor needs to provide:

$$T_{mot} = 0.1\ \mathrm{Nm}, \Omega_{mot} = 650\ \mathrm{rpm}, P_{mot} = 6.86\ \mathrm{W} \tag{4.8}$$

where the gearbox efficiency was assumed to be 60% due to exposure to cold.
In this calculation, mechanical friction losses were neglected, however since the worst-case scenario has been considered (the speed drops considerably when in flight as well as a double weight of the load), it can be easily compensated by the motors currently used in the design (they have a rated power of 7 W each).

4.1.4. Reinforcing connections between various systems

Most of the components used in the design are boards with a fixed type of ports and connectors which cannot be modified for reinforcing these against vibration and shock. Therefore, a reinforcement metal strip, secured using two screws and pinning down the connector is going to be used like in Figure 4.54 for example.

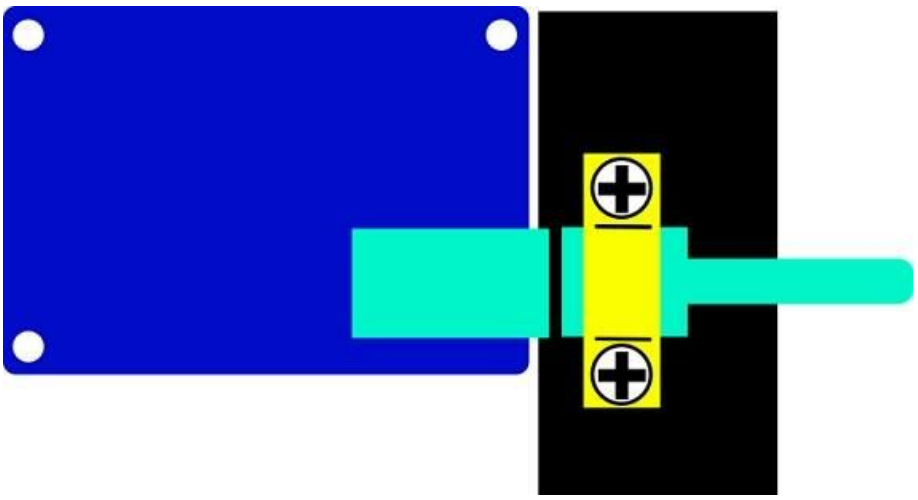

Figure 4.52. – Proposed reinforcement for connectors and ports.

A challenging issue is the ribbon like cable between camera and raspberry pi board. Not only is the cable not long enough, but it is not very reliable when it comes to twisting or protection against cold. Therefore two adapters are used from CSI to HDMI and HDMI to CSI - this means that the same port for the camera is used on the Raspberry Pi, but a much more robust HDMI extension cable is used between the camera and Raspberry Pi. The ends of the HDMI cable are secured in a similar fashion like in the Figure 4.54 ; while the ribbon cable is kept secure, can be located inside a protective case and will not be twisted anymore as the stress is moved to the HDMI cable extension.

Given concerns addressed with regards to wiring and connections during presentations at the training week at DLR-Oberpfaffenhofen, the internal wiring between all elements located inside the aluminium box will be following a single path per level (as shown previously the box is divided into several levels) which will make extensive use of cable ties and will additionally be screwed in several key areas, although there are not high vibrations expected since the described experiment will fly on HASP.

Finally, as pointed out in previous sections, most connections from the experiment to the aluminium box inside the gondola will be joined and passed through the Amphenol 62GB series connector ensuring a high degree of reliability.

4.1.5. Thermal design

Every component inside is susceptible to malfunction making it difficult to design an electrical system which will work during direct exposure to the low temperature. Therefore, the electrical system is insulated inside a box coated with a PE insulation foam. Ideally the temperature inside the box should be -10 °C to 0 °C. There is a heating source present inside the box due to Joule losses in various components - this source (excluding the motors) should be between 34 - 42 W. Future models to estimate the temperature distribution inside the box should consider the 3D aspect of the problem - furthermore the heating sources are distributed inside accordingly to various chips located on the few boards considered. The telescope operation might be affected due to specific phenomena like thermal contraction thus introducing errors.

There are two main systems to consider: outside the gondola, and inside the gondola. Inside the gondola, irradiance is assumed to be 0 Wm^{-2}, while outside irradiance is 1200 Wm^{-2}. The temperature inside the gondola is warmer at -60 °C than outside which is at -80 °C. The ambient

pressures both inside and outside the gondola are the same, at approx. 5 mbar. These figures are valid for an altitude of 25,000 m. During the pre-launch phase the preparation of the payload is done at a temperature of 20±5 °C. The outdoor temperature at the launch pad in Sept/Oct is normally between 0 °C and -15 °C. During the flight phase, the thermal environment of the flight might have an external temperature of -80 °C. At the post-flight phase, the payload will be subjected to temperatures between 0 °C and -15 °C. [3]

The experiment shall operate at a temperature range of -80 °C to 25 °C, and a pressure range of 0 to 100 mbar. While the operating temperature could be at -80 °C, this may affect the mechanical properties of the material.

Motor casing will enclose Sun radiation protection in its design. If the canvas is on top of the gondola, no radiation protection should be considered for the electronics box.
Aluminised Mylar will be wrapped around the telescope assembly and cables to prevent overheating due to the sun radiation.

Table 4.1.4.1 - Component temperature range

Component	Operating T (°C)		Survivable T (°C)		Comments
	Min	Max	Min	Max	
ZWO ASI120MM (mono) Camera	-45	N/A	-60	N/A	A very sensitive piece of equipment
Raspberry Pi	0	70	-82	85	RPi is ideally made to work in the conditions of 0 °to 70 °C, however it has been proven to work under -82 °C as well as the AP (Application processor) i.e. the Broadcom BCM2835 is operable in extremes however performance must be considered when operating under such circumstances
RPi camera	0	70	-82	85	These are not provided in the datasheet, so we assumed they are similar with the Raspberry Pi ones
DC/DC Converter	-40	85	N/A	N/A	-
Gimbal	-80	30	-80	40	Depending on the choice of material for the manufacturing of the gimbal, different temperature ranges can be expected, but they all can safely operate under the following range: -80 - +30 °C
Harmonic drives: HFUC-20-2UH	0	60	-40	90	Space saving gear with operation at -80 to 240 °C possible using special lubrication.

ZFE-60ml Flexolub-M0	N/A	N/A	-70	150	Drop point according to DIN ISO 2176 is > 250 °C. It has a density of 0.98g/cm^3 at 20 °C
Stepper Motors	-18	70	N/A	N/A	Motor enclosure to be insulated with 3cm of white PE foam outside. Additional layer of aluminized mylar will surround this to reflect radiation.
Krytox GPL 203 Grease	-60	154	N/A	N/A	-

4.1.6. Harmonic drive

Figure 4.1.5.1 shows the dimensions of the harmonic drive. The tables following that detail the specifications http://harmonicdrive.de/mage/media//catalog/category/2014_12_ED_1019644_HFUC_2UH.pdf

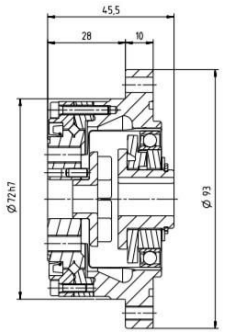

Figure 4.1.5.1 – Harmonic drives - technical drawings

	Unit	HFUC-20-2UH					
Ratio	i [ ]	30	50	80	100	120	160
Repeatable peak toque	T_R [Nm]	27	56	74	82	87	92
Average torque	T_A [Nm]	20	34	47	49	49	49
Rated torque	T_N [Nm]	15	25	34	40	40	40
Momentary peak torque	T_M [Nm]	50	98	127	147	147	147
Maximum input speed (oil lubrication)	$n_{in\,(max)}$ [rpm]	10000					
Maximum input speed (grease lubrication)	$n_{in\,(max)}$ [rpm]	6500					
Average input speed (oil lubrication)	$n_{av\,(max)}$ [rpm]	6500					
Average input speed (grease lubrication)	$n_{av\,(max)}$ [rpm]	3500					
Moment of inertia	J_{in} [x10^{-4} kgm^2]	0.193					
Weight	m [kg]	0.98					

Figure 4.1.5.2. – Harmonic drives -parameters

4.1.7. Motors

Engineering drawings of the motors that are to be integrated in the current design can be accessed at: https://www.oriental-motor.co.uk/media/images/640_ia_pkp5-42mm-highresol-dim. jpg. The motor model is PKP546MN18A.

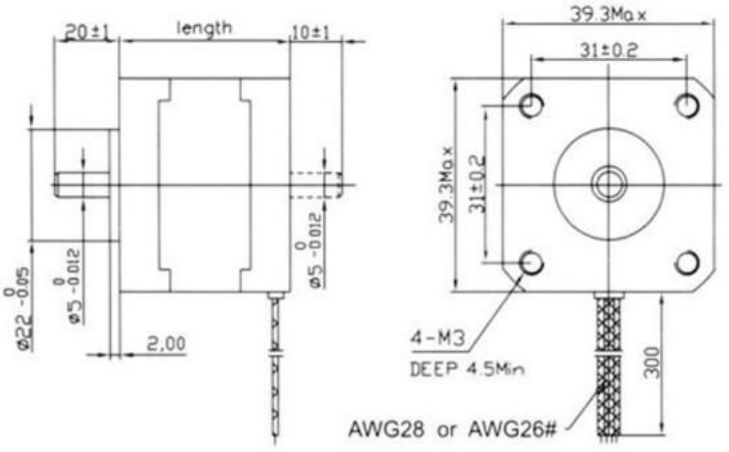

Figure 4.1.6.1. – Motor structure drawings

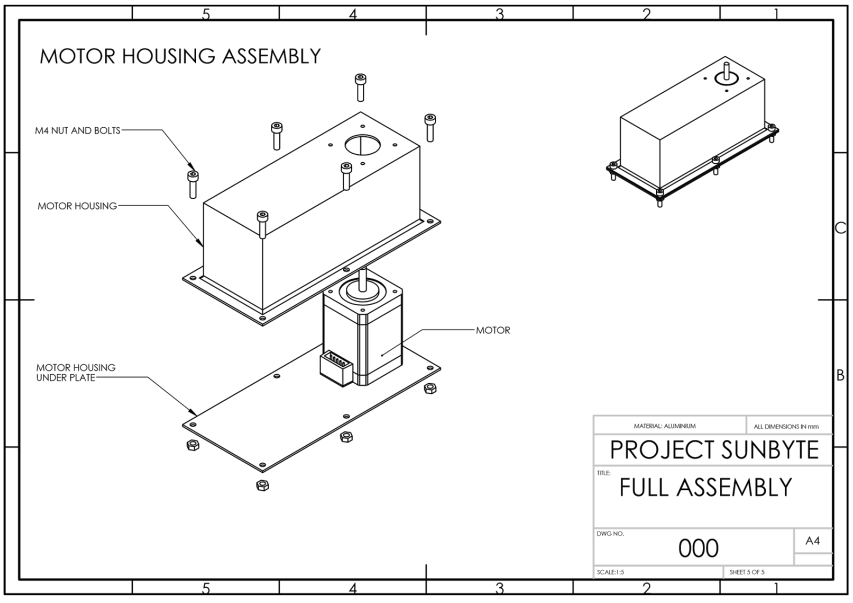

Figure 4.1.6.2. – Motor Housing Assembly Drawing

4.1.8. Optics

The chosen focuser is the TS-Optics 2 ”Helical Extractor Screw Focuser” which uses an M48 connector. It is capable of an adjustment distance of 39mm and precise focusing of up to 1/20 mm accuracy. This was chosen as the inner tube does not rotate thus allowing the orientation of the camera to be retained. Two fixing screws hold the focus position.

Figure 4.1.7.1. – TS-Optics 2 Helical Extractor Screw Focuser

The focuser will be lubricated using Krytox GPL 203 grease, which is suited for cryogenic conditions of down to -60 °C. A gear wheel will be fabricated to fit over the knurled area. Adapters are required to set the correct distance from the telecentric to the etalon. The focusing design used for the camera not only acts as a way to automatically control the focus of the camera but to also support the mass of the camera. The design allows for the bigger gear fitted around the focuser to increase and decrease in length while still being attached to the smaller driving gear due to the length of the smaller gear. The design also adds support to improve the stability of the camera by fixing the smaller gear directly to the camera and fixing the smaller gear to a shaft which slides in and out of a hole fixed to the telecentric clamp. Doing this not only stops unwanted movement from the small gear but also the shaft and telecentric clamp configuration acts as a pivot to support some of the weight of the camera.

4.2. Electrical

4.2.1. Image detection

Getting into more details the image detection algorithm would raise the question of the amount of light and the exposure time required to achieve reliable performance in Sun's detection. This would ideally have to be correlated with the following steps (especially no. 3):

1. Obtaining the information (the 'R', 'G', 'B' value) of a range of pixels collected from the upper half of the image.
2. Using the data above to calculate the luminance.
3. Assign a luminance threshold, such that values above it would correspond to space atmosphere, and the values below would correspond to below stratosphere environment.

In order to deliver a proof of concept experiment, initial tests were conducted on the algorithm based on static stock images as input. Reasonably good results in both space and terrestrial environments were obtained. For example, the space environment results were obtained by processing stock images of the Sun captured in outer space. The success of the algorithm was appreciated by its ability to separate the Sun's shape in all available stock images. The results can be observed in Figure 4.2.1.1. and 4.2.1.2.

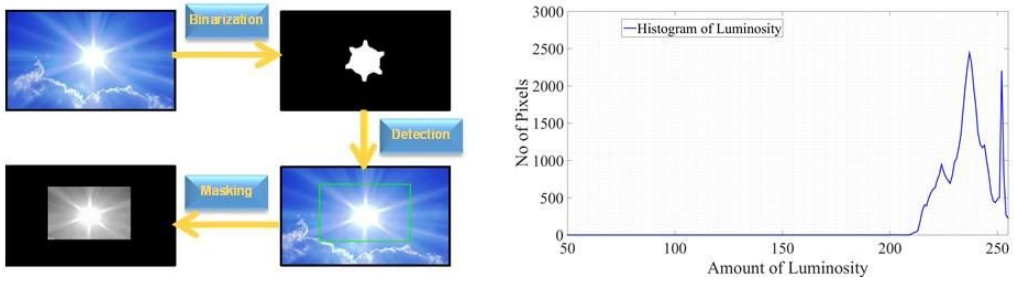

Figure 4.2.1.1. – Proposed algorithm running on daylight.

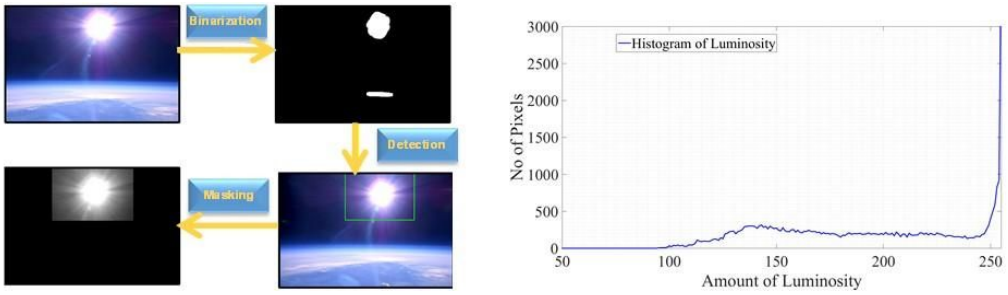

Figure 4.2.1.2. – Proposed algorithm running in upper atmosphere.

As for the method's limitations, these stems from lighting conditions available to the Sun tracking camera. We can see from the results above that if the light amount reaching the camera is **in a comfortable range** (i.e not too bright not too dark), the binary image of the Sun would appear as roughly a circle and hence would be manageable by the shape detection algorithm. Despite tests being performed in both Sunlight and stratosphere environments a clear distinction of Sun shape based on number of pixels being in the majority in the bright region of the histogram (i.e. the right-hand side) was always obtained. However there is a reason for concern shown in the first figure as an over-bright (overexposed) input can lead to production of a **'distorted shape'** (as illustrated in the binary image). It is not possible to infer that there is a circular shape in the brightest region of Figure 4.2.1.1.

It can be concluded that there is a good chance that higher number of pixels in the bright region (i.e. large area to the left hand side of histogram to with luminosity < 200) can lead to shape distortion which would prevent shape detection algorithm to continue with obtaining the centroid of the Sun.

The initial results are encouraging however, more robust methods need to be tested. In order to improve the results, improvements have been made in the form of canny edge masking which allows trails of Sun to be detected once the computer vision algorithms are run.

4.2.2. Image focusing

As the environmental conditions change the focus of the telescope will vary due to strain on the structure and temperature related material contraction, this can be corrected by regularly refocusing the telescope which requires the imager to be mechanically moved forwards or backwards parallel to the telescope tube.

With the uplink bandwidth being limited, a live video stream is impractical and so manually focusing is impossible during flight.

An automatic software-based solution has been developed by the software team that is designed to operate completely independently of the operators.

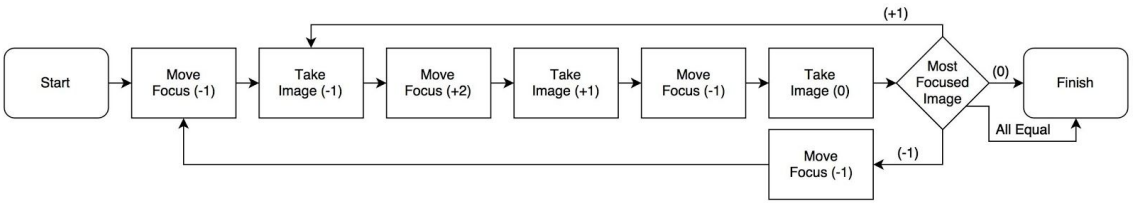

Figure 4.2.2.1. – A flowchart of the basic focusing implementation.

With this method, the system repetitively attempts to adjust the focus and check if the changed focus (moved one increment forwards or backwards) is better than the final resting position. The final resting position is expected to be close to the initial position, but the image is taken last to ensure there is no drift when trying to return to that position. The algorithm is not the fastest possible when the focus is too far off at the start of the process, as the system will need to repeatedly move backwards and forwards through the focal plane in small increments, however the telescope is expected to be focused on the ground and only need to maintain focus thereafter.

Focusing times. The focusing process is to be automatically undertaken at regular intervals, expected to be every 10 minutes but to be determined in testing.

During the focusing intervals the main telescope camera will be collecting data as normal and these images will be used to as the images to compare for focusing.

Additionally, a text log of the focusing times will be recorded to the main SSD to help in the removing of blurred images during post-processing.

Note: if the scientific camera is no longer acquiring images then improving focus will not be possible, instead the comparison will generally be of the latest image to itself and the process will terminate as it determines the current focus is as good as the other 3.

Testing focus. The focusing process requires a method of comparing the focus of 3 images and determining the sharpest (best focus) of these. The Sun, as a very strong light source, gives a very

high signal-to- noise ratio making sharper focus lead to a higher dynamic range in the image, this can be used as a basic metric for focus.

The method involves taking the maximum intensity value (I max) and subtracting the minimum intensity value (I min) to get a quantity for the dynamic range. The highest value of dynamic range will generally correlate to the most focused image, see Figure 4.66

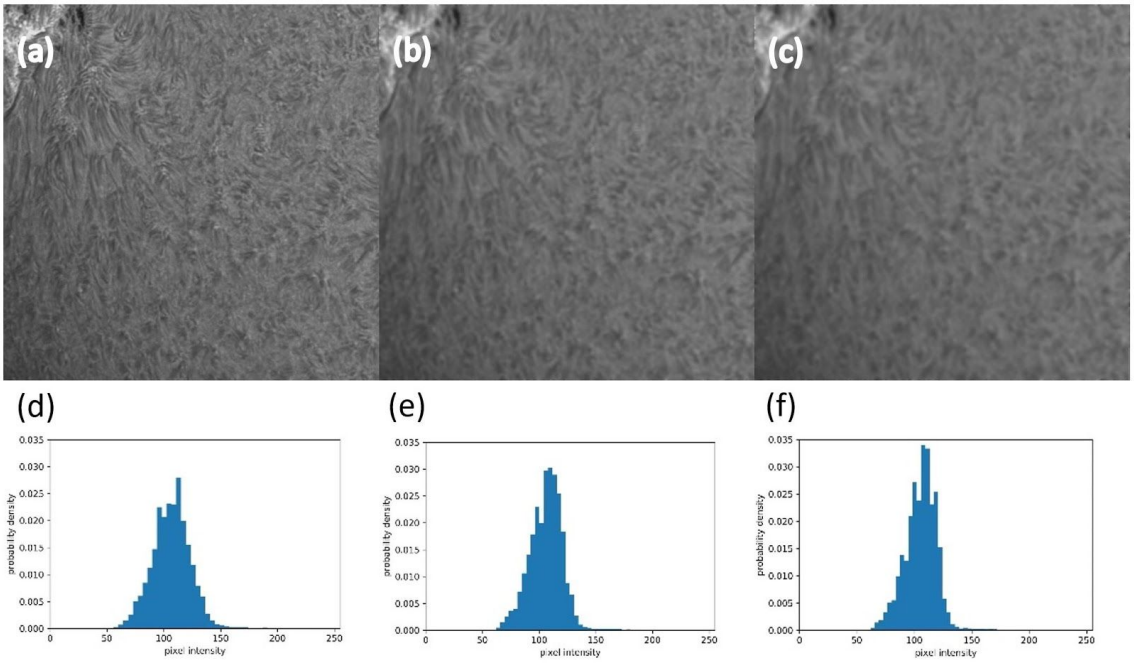

Figure 4.2.2.2 – An initial H-alpha image (a) is filtered with a basic blue once in (b) and twice in (c), the resulting dynamic ranges are 211, 192 and 184, showing that (a) is recognised at the best focus.
The histograms of (a), (b) and (c) are given in (d), (e) and (f), as can be seen, the increased blur tends to spread the range of intensity values towards high or lower values, leading to a higher dynamic range.

4.2.3. Motion blur

An additional source of blur other than incorrect focus can be if the telescope is in motion, this will cause a motion blur as the camera sweeps over an area during the exposure. Exposure times are expected to be at maximum 1/40 s (limited by the capture rate of the imager) and are likely to be substantially less due to the large aperture of the telescope providing a lot of light to measure. However, an additional control step will be added to the focus process to check if the projects accelerometer is detecting motion above a given threshold, if-so then a new image will be used for the focus reference at the given focus.

Full process. The resulting process adds a check for motion and waiting delays to allow the motion to settle down. This is simple to represent in a flowchart.

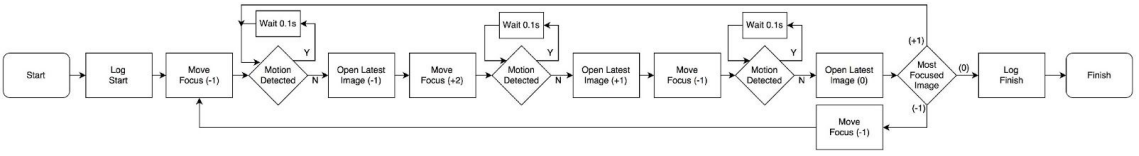

Figure 4.2.3.1.. – A more comprehensive flowchart of the focusing process.

Consideration has been given to the possibility the telescope will under constant motion, in this case the telescope will be constantly waiting before it can adjust the focus. This won't interrupt the data acquisition and so is considered to be graceful degradation of functionality. Ground control over the motion threshold may be added to allow us to correct mid-flight if this is too sensitive.

Similarly, additional functionality can be added to change the focus adjustment distance increments if the system it too far out of focus to be able to return quickly enough, or in the event the small increments don't provide enough of a change to the dynamic range to allow focus.

4.2.4. Image processing

The purpose of this subsection is to roughly present an overview of the data acquisition software characteristics. This is based on the high-tech camera provided by Andor which will capture images directly from the telescope. It will run on top of a GNU/Linux based operating system due to its highly customisable characteristics. In terms of functionality it will provide the following:

- compress the raw images generated by the Andor camera to a suitable lossless format (for example zipped binary files) and write them to the available storage;
- run in batch mode to increase the speed and remove the unnecessary overhead. There will be no GUI for example;
- optimise the processes and make sure the ones required by task at hand gets maximum priority;
- configure the appropriate functionality (i.e. establish the connection with Andor camera, during the startup sequence) which should be used whenever the computer (re)starts; • provide a log of the current events (i.e. "image acquisition starting at ...") with basic diagnostics to test it pre-launch;
- only fire the Andor camera when the telescope is aligned with the Sun (i.e. no unnecessary data will be processed and stored - no blank images).
- generate external diagnostics signal (i.e. 'alive' signal) to communicate its current state to monitoring controller

The actual implementation relies on Andor SDK which is written in C++ and also available on Linux. The camera can take pictures with up to 40fps, however for the success of the experiment, this feature is not required. A list of steps defining a typical C++ program based on Andor SDK which acquires images is represented below:

1. Launch and initialize the Andor functionality - (AT InitialiseLibrary());
2. Open a connection with the camera (AT Open (int i cameraIndex, AT H Hndl) where the i cameraIndex is the index of the camera known a priori. The function returns a handle Hndl which allows accessing various camera states;
3. Set memory aside to accommodate the incoming images from the camera AT QueueBuffer(AT H Hndl, unsigned char* pucAlignedBuffer, AT 64 ImageSizeBytes) - the ImageSizeBytes specifies the amount of memory to be allocated while pucAlignedBuffer is determined before and required for a byte offset alignment which increases the performance

4. Start frames acquisition, dump data to disk, end aquisition - AT Command(Hndl, L“AcquisitionStart”) - the SDK does not provide functionality for writing or converting images into various formats - this will be provided separately. The aquisition ends with AT Command(Hndl, L“AcquisitionStop”);

5. The program ends with AT FinaliseLibrary( ) call which releases any resources currently in use.

4.2.5. Testing

In the electrical part of the project there has been a constant progress with regards to testing. Since the final devices were not available, control of the motors has been tested by use of available components. Some of the employed are pictured below including L298N drivers and stepper motors with 1.8 degrees per step together with a simple connection example.

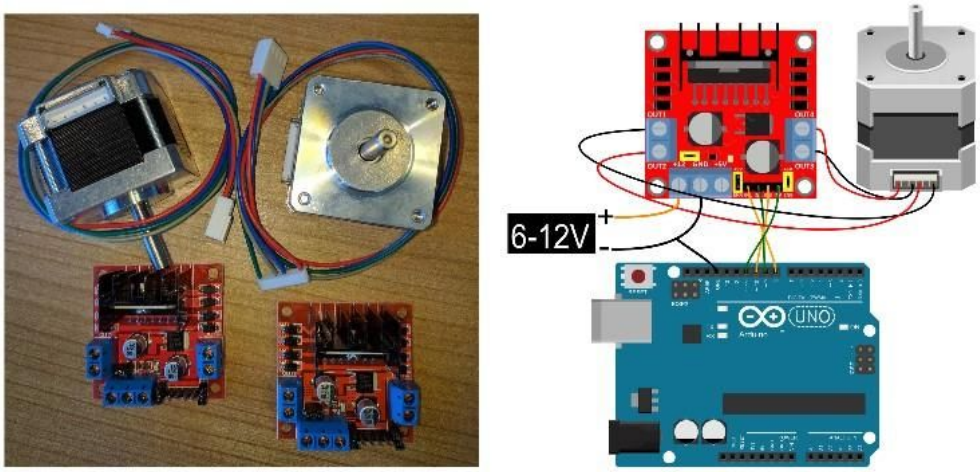

Figure 4.2.5.1. – Actuator motors and their drivers

Testing using these tools offer a lot of information about performance of control software built for Arduino, power consumption of the motors, relation between voltage available and maximum achieved speed and required torque and thus current drawn. The motors are controlled by the drivers which are themselves controlled by the Arduino.

As seen below, testing has been performed by use of a first gimbal prototype that allows two axis of rotation and already incorporates one of the cameras currently under consideration.

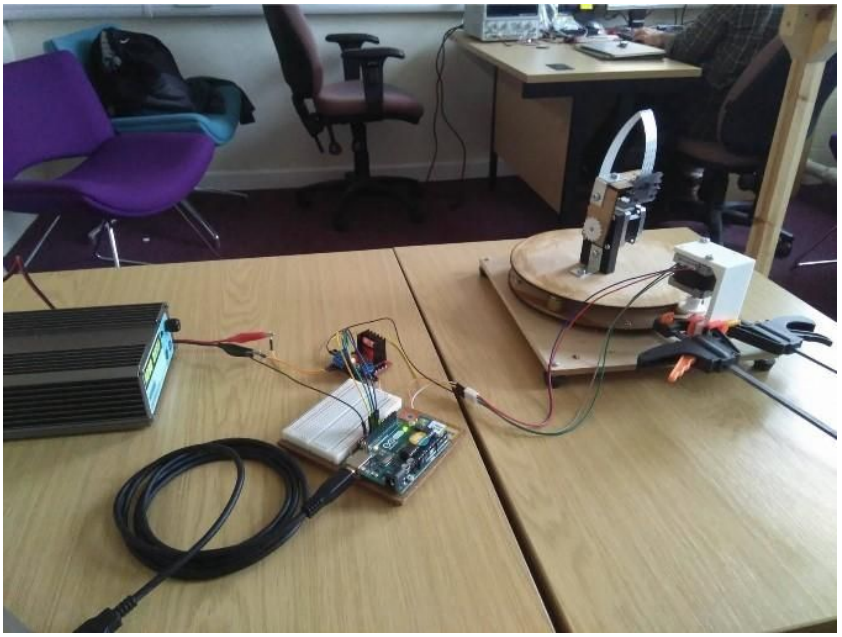

Figure 4.2.5.2. – Gimbal Prototype 1 interfaced with Arduino. Video is available here: http://sunbyte.group.shef.ac.uk/galleryv2.html)

Performing these tests allow us to get an insight into the behavior of our motors. The software located in the arduino is ultimately in charge of correcting the aim of the telescope for which a communication is needed between the Arduino and the Raspberry Pi where the sun tracking algorithm is running. For that purpose, the Arduino is constantly ”listening” for commands that allow a two axis error compensation. Additionally, the possibility of controlling the motors directly from the Raspberry Pi seen in the following figure has also been studied with satisfactory results. Videos of these tests are available on the team website.

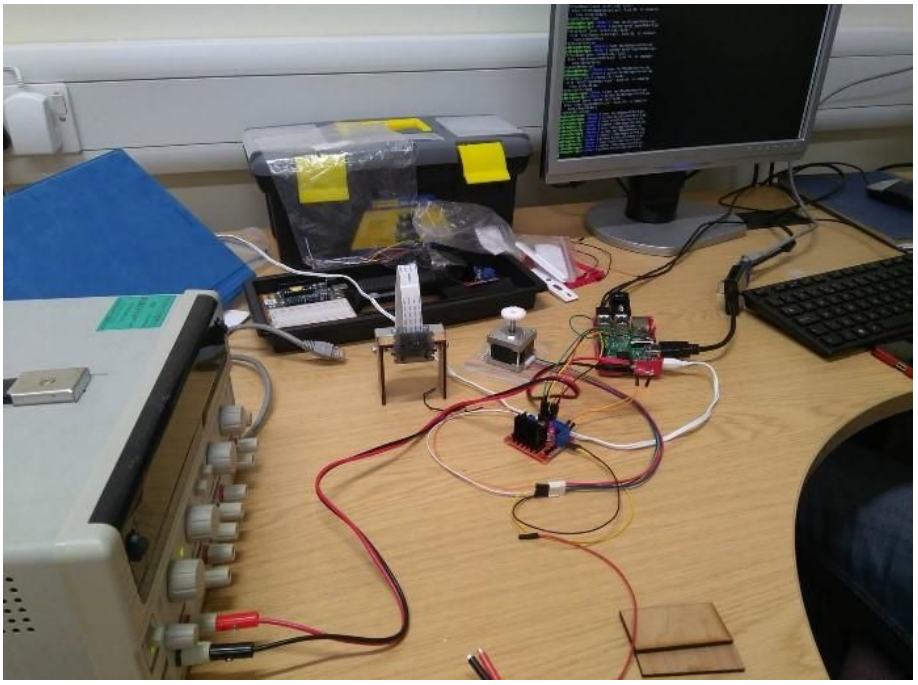

Figure 4.2.5.3. – Actuator motor controlled from Raspberry Pi. Video is available here: http://sunbyte.group.shef.ac.uk/galleryv2.html

Following testing on the first prototype, a second version of the gimbal was built, shown next, this time mounting a real telescope with the possibility of attaching our SCMOS camera.

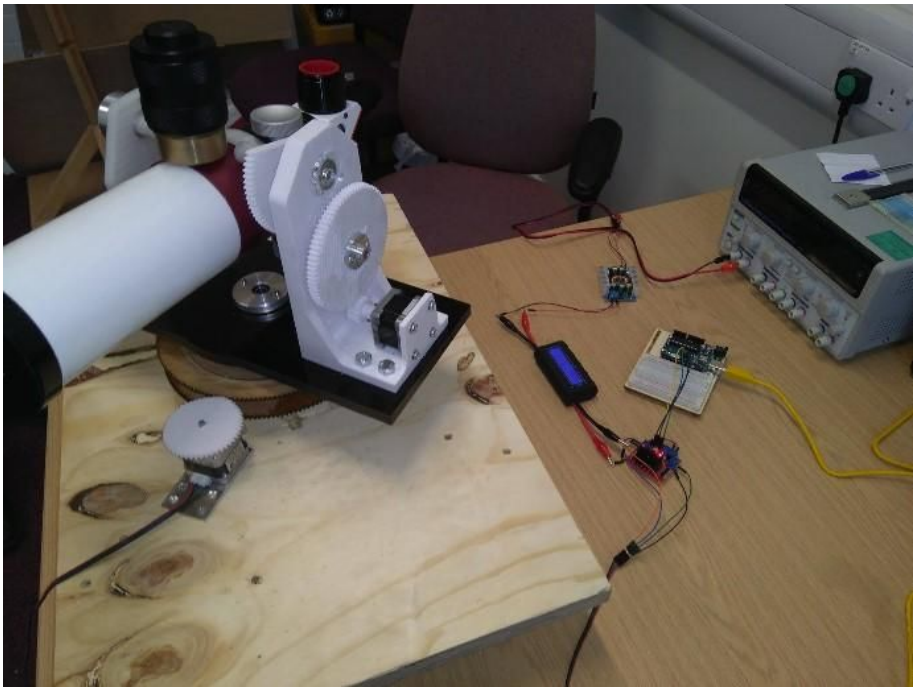

Figure 4.2.5.4. – Gimbal prototype two

A closer look at the right part of the figure allows seen that control of the motor during testing is being carried out with all elements associated including DC/DC converter, wattmeter for power consumption and driver. A zoom in of this section is presented next:

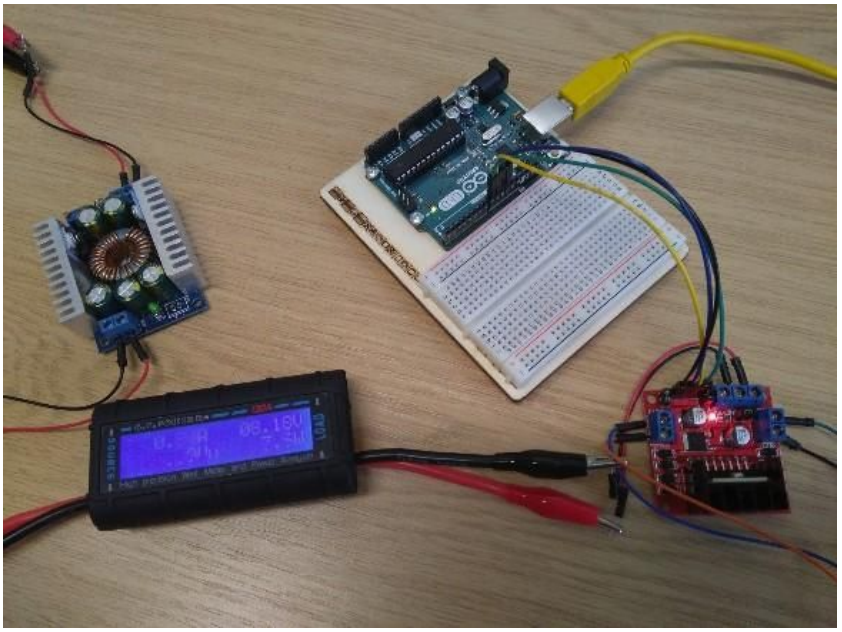

Figure 4.2.5.5. – Electronics associated with driver during test.

Finally, a last prototype has been built out of already available Lego with the aim of simplifying further testing, releasing the motors of a relatively high torque demand, lightening the testing platform and allowing the use of extra elements already available as well as lower power motors/drivers.

Figure 4.2.5.6. – Third gimbal prototype made out of Lego.

It is possible to see that for the third gimbal, seen on the figure above this lines, the pi-camera has been integrated, easy to spot due to the white ribbon connector. This last gimbal model presents no reduction apart from the internal gearing of the motors, given that the motor shaft is directly connected with the axis of rotation. The final aim, being a fully functioning two-axis actuation of the gimbal has been achieved, and more importantly, commands are given directly by the raspberry-pi as a result of execution of the sun-tracking algorithm. This Lego gimbal prototype has been presented at an outreach event for the UK Pint of Science 2017.

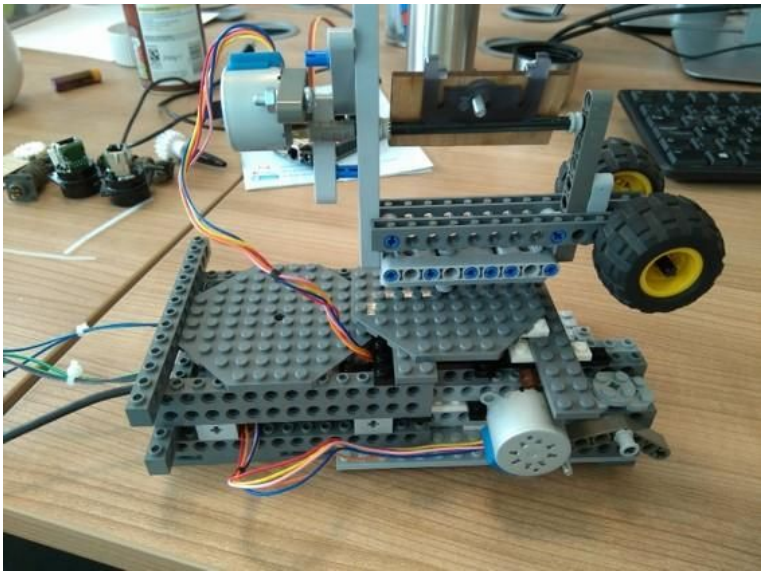

Figure 4.2.5.7 – Fourth gimbal prototype and second made out of Lego

The final iteration of Lego gimbal prototype is presented in Figure 4.2.5.6. In this case a solid platform has been built and a gear reduction (40/8) has been included to improve the accuracy of even quick tests and to present a more experiment-wise prototype for outreach. This gimbal prototype has been presented at the ”IET Present Around the World - Northern Area Final”, at Preston, June 14th.

Testing of the Stepper Motor and Driver

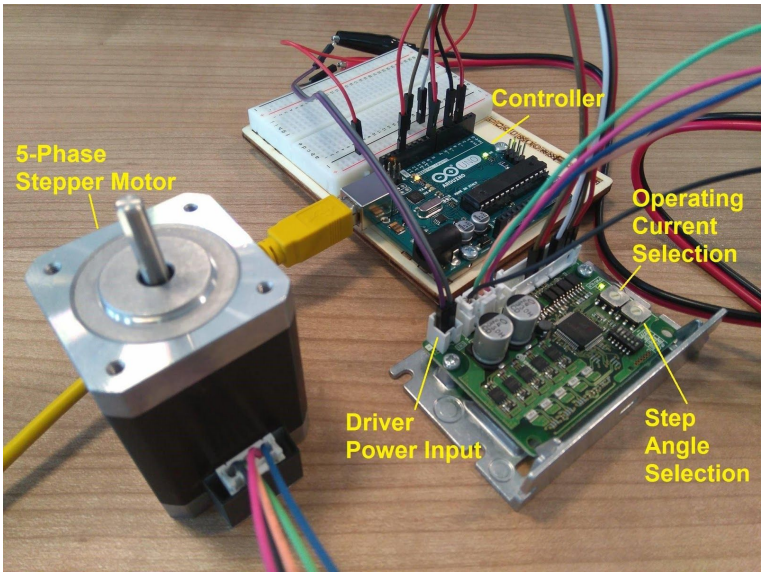

Figure 4.2.5.8. – Stepper motor and driver

Testing of the chosen stepper motor and driver are shown in Figure 4.2.5.8. The selected driver allows performing microstepping without the need of additional circuits or code. All that is needed is to select the step angle for the microstepping and set off port 7 (CS - Step angle switching input) of the Driver CN3 (I/O signals) as seen in Figure 4.2.5.9.

■ Connector pin assignment

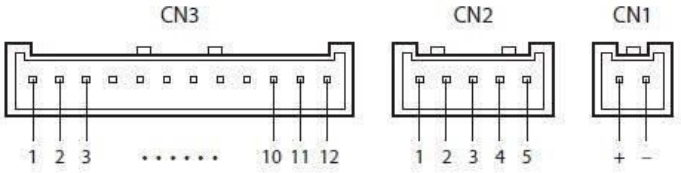

● CN1 (power supply)

Pin No.	Direction	Signal name	Description
+	IN	POWER	+24 VDC
–			GND

● CN2 (motor)

Pin No.	Direction	Signal name	Description
1	OUT	MOTOR	Blue motor lead wire
2			Red motor lead wire
3			Orange motor lead wire *
4			Green motor lead wire
5			Black motor lead wire

* This orange lead wire is for 5-phase stepping motor. For 2-phase stepping motor, do not connect anything to the pin No.3 since there is no orange lead wire.

● CN3 (I/O signals)

Pin No.	Direction	Signal name		Description
1	IN	PLS (CW)	+	Pulse (CW pulse) input *
2			–	
3		DIR (CCW)	+	Rotation direction (CCW pulse) input *
4			–	
5		AWO	+	All windings off input
6			–	
7		CS	+	Step angle switching input
8			–	
9	OUT	ALM	+	Alarm output
10			–	
11		TIM	+	Timing output
12			–	

Figure 4.2.5.9. - I/O pins

Given that the microstepping position needs to be fixed at a certain value of step angle for the entire duration of the flight, there will only be two modes of operation available, the default step angle of 0.36 degrees per step and another one, between the minimum needed of 0.036 and 0.00288 degrees per step. This selection is based on a tradeoff between the accuracy needed to meet our requirements and the speed needed to compensate for the rotation of the gondola. Maximum speed achieved so far is 130rpm, considered enough to meet our requirements.

4.2.6. Sun position estimation by means of photoresistors:

As explained before, an array of photoresistors was being considered as a possible back up solution in case all Sun tracking and position systems fail. On its most basic forms it was to be formed of 6 elements connected to 6 analog ports of the Arduino and placed in a frame shaped like a hexagon.

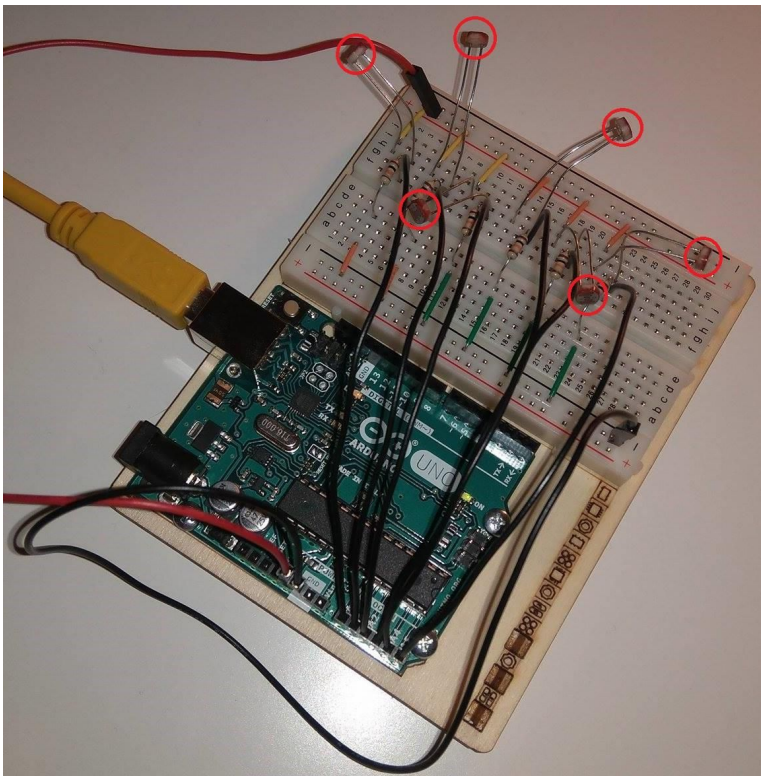

Figure 4.2.6.1. – Photoresistor array test.

The way it was carried out was by computing the analog magnitude of the resistance read from each photoresistor and comparing it to the rest. In this way, if one read was far superior from the rest it was possible to assume that the S un position was in the vicinity of that element (60°), if it was almost the same in two elements will be located in between them (30°), and if it was higher in one, closely followed by another it was possible to assume it was in the closest 15°starting from the first and towards the second. To compute a higher degree of accuracy with just 6 photoresistors seemed out of reach. The possibility of using far more than 6 elements was also available given the choice of Arduino MEGA as microcontroller platform (16 analog inputs) but the need to shield them from the outside environment, a large amount of extra wiring and the extra computational load resulted in not pursuing this method.

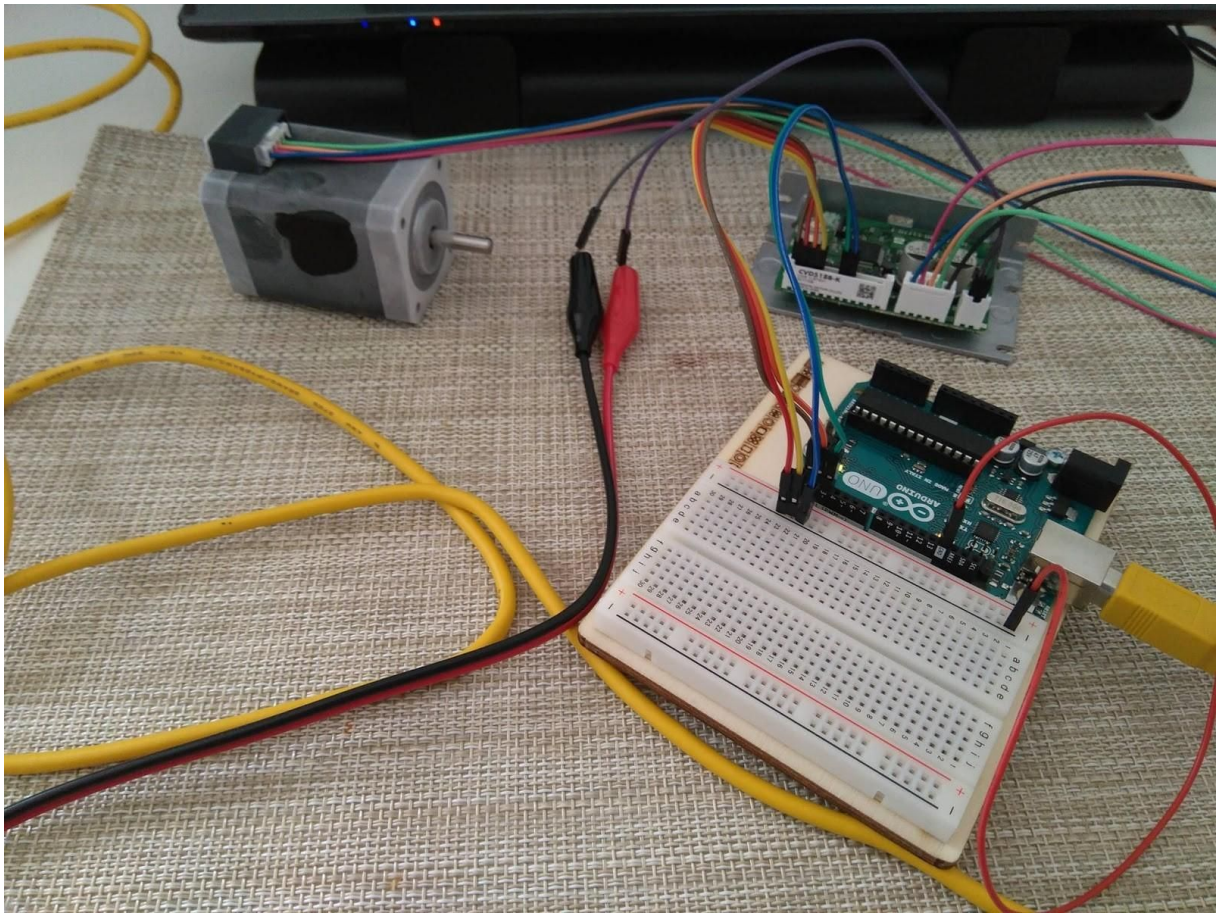

Figure 4.2.6.2. – Cold Test

The motor and driver were placed in a freezer and allowed to cool for 2 hours until a temperature of 18 degrees Celsius was reached. They were tested immediately after and were still functional.

4.3. Software

4.3.1. Sun Positioning System

First stage Sun tracking using astronomical calculations have been prototyped using LabVIEW. The output of the algorithm was first tested by comparing results to NOAA Solar Position Calculator [10] and the results matched.

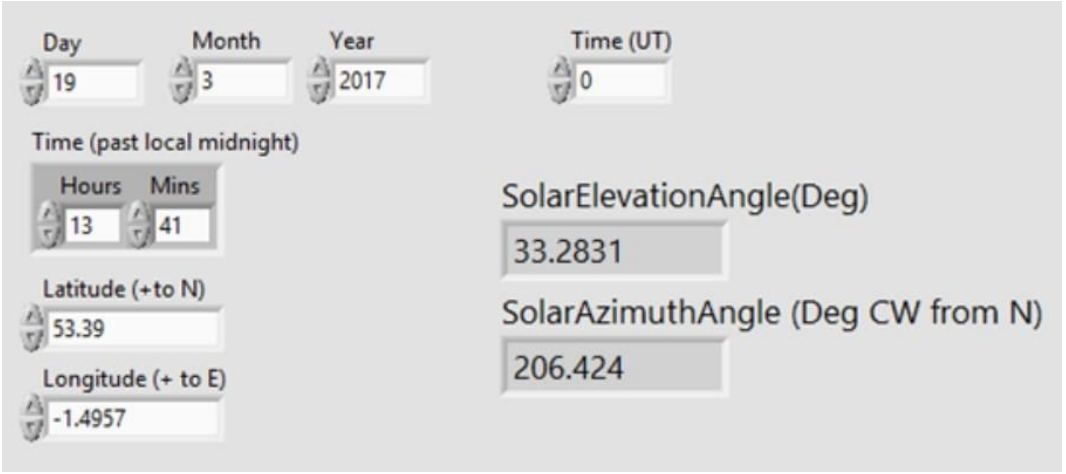

Figure 4.3.1.1. – Sun Locating based on Astronomical calculations, LabVIEW program front panel.

Furthermore a simple hardware prototype was built using two servo motors attached perpendicular to each other to represent the Azimuth and Elevation angle as shown in figure below. The prototype was tested on a sunny day and give very satisfying results and could track the Sun with a relatively small error of +/- 2 degrees.

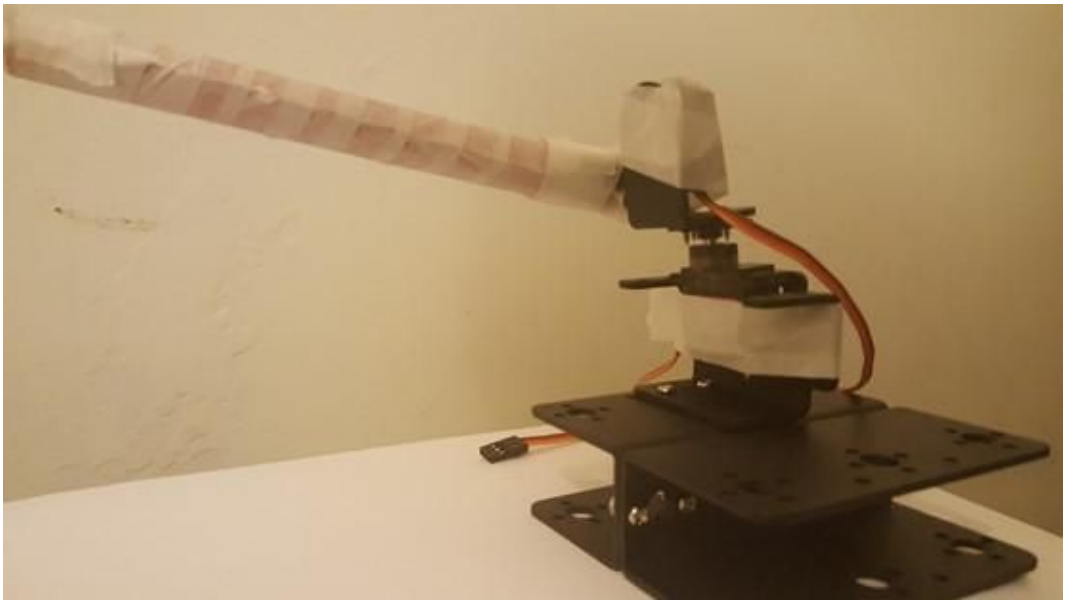

Figure 4.3.1.2 – Sun locating simple hardware prototype using servo motors.
Video is available here: http://sunbyte.group.shef.ac.uk/galleryv2.html.

Thus the concept was proven to work and this method is the primary choice to be used in the first stage tracking. Other methods are investigated as well. Currently, this algorithm was ported to Python and awaits integration with the stage two algorithm.

4.3.2. Sun Visual Tracking System

Experimentation with Tennis Ball

Due to the lack of data set at the time being, the experiment for the visual tracking system was performed on a tennis ball. The main idea was to ensure whether the algorithm was capable of running smoothly and be able to track a circular object with ease. The following result was obtained. The red trails indicate the location of previously stored results i.e. the past visiting instances of the ball. However point to be noted is that this info is rather superfluous for actual test where storing past instances would be unnecessary and rather consume more of precious memory. But that is unless the velocity would be required to be calculated but that again would be unnecessary because the on-board IMU sensors are more than enough and much more accurate than vision based speed inferences. This leads us to the discussion of the difference between projectile deviation vectors (PDVs) and centroid deviation vectors (CDVs). The CDVs, by virtue of the name, tells us the horizontal and the vertical distance (cX, cY respectively) of the centroid of the ball to the centroid of the tennis ball. On the other hand, the PDVs tell us the displacement from the last known position to the current position and can be used to calculate the velocity.

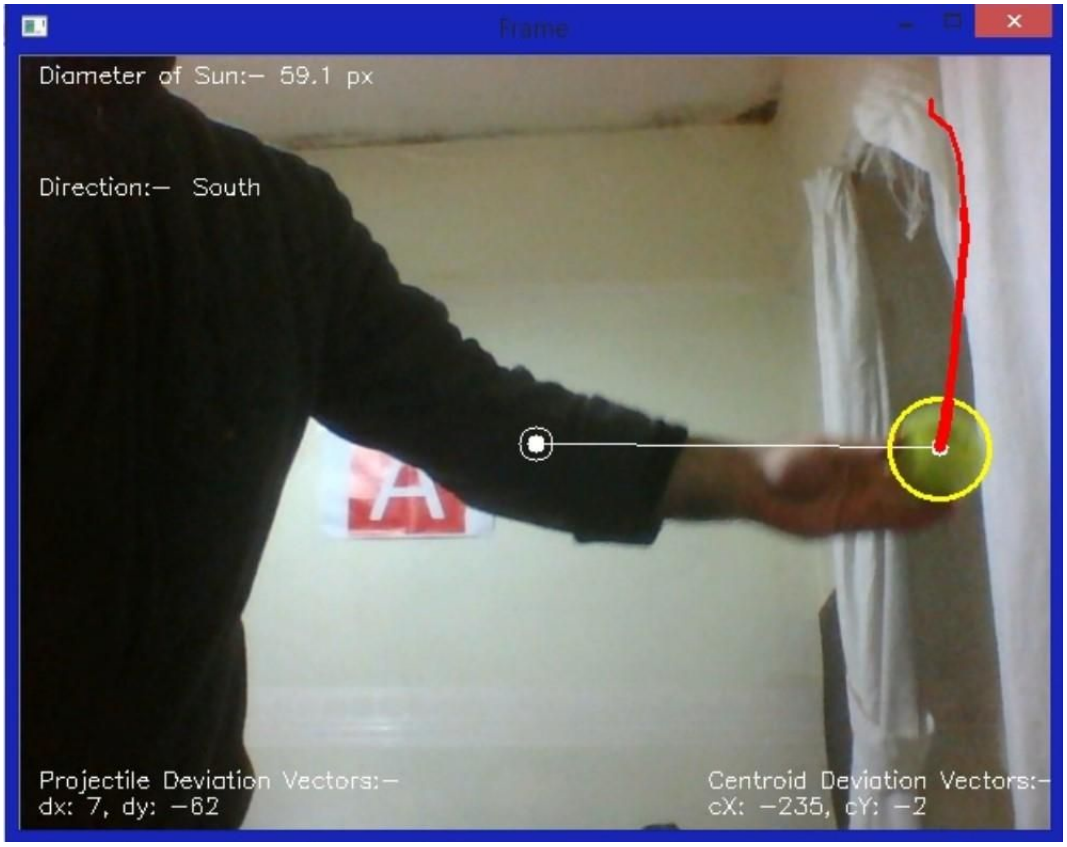

Figure 4.3.2.1. – Visual tracking algorithm tested on a tennis ball prototype.

Experimentation with Capture Dataset

With dataset captured from one of the software team member, the algorithm tested on the tennis ball as shown above was made to test on the data captured and the following result was obtained. The dark background was achieved using neutral particle density filter.

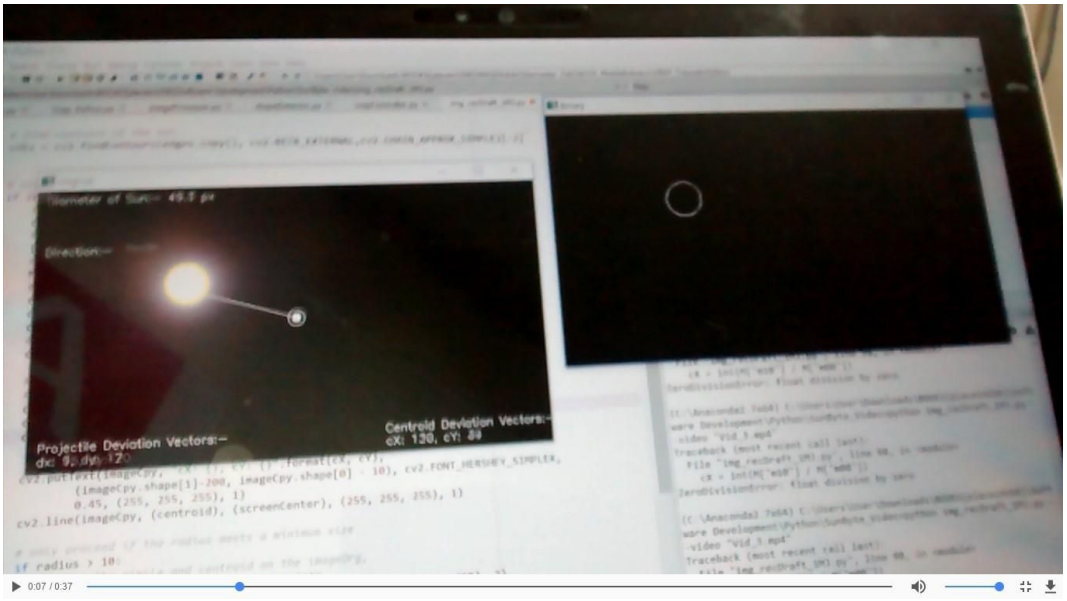

Figure 4.3.2.2. – Visual tracking algorithm tested on dataset Please see the entire. video on our website :http://sunbyte.group.shef.ac.uk/galleryv2.html

Testing the 360 degrees camera with Raspberry Pi and OpenCV

The raspberry pi was associated with a 360 degrees cameras (RICOH Theta), obtaining a two fisheye live stream at a satisfactory frame-rate. This was not pursued further (i.e. the image processing algorithm was not adapted) as we already have an acceptable solution for first stage tracking.

Figure 4.3.2.3. – Sample output from the 360°camera

5. Data analysis and Results

5.1. Data Analysis Plan

One simple way to assess the quality of the images is to estimate the Fried parameter (otherwise known as r_0) which is a measure of ”seeing” in astronomical circles. Most ground-based observatories use this to monitor the level of atmospheric turbulence in real time. The Fried parameter has units of length and is typically expressed in centimetres. It is defined as the diameter of the circular pupil for which the diffraction limited image and the seeing limited image have the same angular resolution. So telescope images with apertures smaller than this parameter are less affected by seeing effects than diffraction due to the small aperture. Telescopes with larger apertures than the parameter are more limited by the turbulence in the atmosphere (seeing). In short, if the desired accuracy in determining the fried parameter is 10% then for a telescope with diameter less than 1m then approx.:

$$r_0(cm) = 1.5* \text{(RMS of the image intensity contrast)} \qquad \text{(Eq. 7.1)}$$

The best telescope sites on Earth have r_0 greater than 200 mm. This calculation could possibly be run in real time in our experiment i.e. to calculate the intensity contrast one could take the mean of the intensities over the image and divide by the image standard deviation over time. The determine the RMS periodically to estimate r_0 as above and monitor that value as a way of comparing between periods of good and back seeing i.e. in real time. The Strehl intensity ratio is another measure of seeing and it is the ratio between the heights of the PSF peak of the actual image and the ideal diffraction limited image. Possibly, this could be attempted in real time on computer on the instrument using a predetermined model of the telescope PSF in controlled conditions.

6. Risk Analysis

6.1. Safety Risks

Risk	Key Characteristics	Mitigation
Sharp edges, machined Aluminium	Sheet and tubing, some sharp edges exist after machining.	Deburr edges where possible. Contain sharp edges in tough material. During transportation, use protective gloves when handling if sharp edges are still present.
Massive bulky structure	The mass of the assembly poses risk of trapped and damaged digits or feet being crushed.	Order of assembly should be well thought out and practiced. A safe number of people are present during assembly and that there is a dedicated space for assembly.
Motor speed > 10rev/s	During testing motors will be running at over 500 rpm.	Care should be taken to avoid hair getting caught around motor shaft. Long hair tied back.
Batteries exposed to low ambient temperature and pressure	Lithium type based on SAFT LSH20 cells grouped together. Number of : 2	Environmental testing will be conducted. Batteries are approved and provided by ESA.
Parts dropping from gondola	Parts are heavy enough to cause harm if they fall onto people	All parts sufficiently fastened. Testing conducted to ensure fastening is able to hold all parts in place in case of turbulence.

Table 6.1.1. – Experiment safety risks

6.2. Risk Register

Risk ID

TC - technical/implementation
MS - mission (operational performance)
SF - safety
VE - vehicle
PE - personnel
EN - environmental

Probability (P)

A. Minimum - Almost impossible to occur
B. Low - Small chance to occur
C. Medium - Reasonable chance to occur
D. High - Quite likely to occur
E. Maximum - Certain to occur, maybe more than once

Severity (S)

1. Negligible - Minimal or no impact
2. Significant - Leads to reduced experiment performance
3. Major - Leads to failure of subsystem or loss of flight data
4. Critical - Leads to experiment failure or creates minor health hazards
5. Catastrophic - Leads to termination of the HASP programme, damage to the vehicle or injury to personnel

Table 3.2. - Risk register

Risk	Risk and Consequences	Probability	Severity	PxS	Action
TC10	Sun not Found	A	4	Very low	Calibrate the telescope to find the Sun
TC20	Breakage of telescope	C	3	Low	Simulations done on the material to prevent it from breaking
MS10	Sun found but accurate pointing not achieved	B	2	Very low	The telescope calibrated under a light source so that it recognizes the intensity of the Sun
MS20	Telescope not focused	C	3	Low	Change the resolution and refocus
MS30	Motors overloaded	A	2	Very low	Multiple tests run before the launch to check the motor isn't overloaded
MS40	Control boards fail	B	4	Low	Multiple tests run before the launch to check the control boards work
MS50	Hard drives full	B	3	Low	Complete measures taken to ensure the hard drives are empty
MS60	Telemetry fails during focus	C	4	Medium	Recalibrate to refocus
MS70	Outgassing of the 3D printed parts	B	2	Very low	Specific care to be taken during the selection of appropriate materials

Table 3.3.

Risk	Risk and Consequences	Probability	Severity	PxS	Action
MS80	Gears get jammed	C	2	Low	The gears must properly oiled before launch
MS90	Heavy winds might make it disbalanced	D	2	Low	A gyroscope will be used to get alerts for proper orientation
SF10	Parts of gondola fall off	A	5	Low	It is ensured that the all the parts are properly bolted in
EN10	Rays focused on someone due to damage to telescope camera	B	4	Low	Calibration of telescope set properly so that rays do not get misguided
EN20	Short circuiting of the system	B	3	Low	Implementation of a fuse or Mini circuit breaker to stop the system from burning down.
VE10	Side strut breaks	C	3	Low	Analysis of side struss done under excessive weight to make it strong
VE20	Collision of support structure with launching mechanism	B	4	Low	The angle of launching mechanism calculated to prevent collision
PE10	Delay in achieving deadlines due to shortage of engineers	C	3	Medium	Recruitment of able engineers expediently by the management team.
PE20	Unprecedented cancellation of meetings	C	2	Medium	The management team must ensure the timings are appropriate and everyone abides by them

Table 3.4.

Risk	Risk and Consequences	Probability	Severity	PxS	Action
PE30	Lack of skills for use of modelling and analysis softwares	B	2	Medium	Hiring across multiple disciplines using working groups rather than sole experts
PE40	Sudden resignation of members	C	1	Medium	Management team ensure morale remains high through a variety of techniques
PE50	Miscommunication of Information	D	2	Medium	The management team should be responsible for ensuring proper information is conveyed to all team members